

PRODUCTION OF BIOPOLYMER USING A
MEMBRANE-BASED BIOREACTOR

by

Christopher A. Marks

A thesis submitted to the Faculty and the Board of Trustees of the Colorado School of Mines in partial fulfillment of the requirements for the degree of Master of Science (Civil & Environmental Engineering Science).

Golden, Colorado

Date _____

Signed: _____

Christopher Alan Marks

Signed: _____

Dr. Junko Munakata-Marr

Thesis Advisor

Signed: _____

Dr. Tzahi Y. Cath

Thesis Co-Advisor

Golden, Colorado

Date _____

Signed: _____

Dr. John McCray

Professor and Department Head Department
Civil & Environmental Engineering

ABSTRACT

Methane is a potent greenhouse gas produced from natural gas reservoirs, landfills, and anaerobic digesters. Some methanotrophic bacteria produce intracellular polyhydroxybutyrate (PHB) in the absence of nitrogen and presence of methane and oxygen. In this study, Colorado School of Mines (CSM) and Mango Materials (MM) collaborated on a Phase I NASA grant, investigating the production of PHB in a novel membrane-based bioreactor. Direct gas sparging is MM's current method of gas delivery, but one of NASA's potential applications for this system would be in microgravity where gas bubbles will not rise, making mass transport and exchange/resupply of gas almost impossible. Membrane contactors may be a management solution for liquid and gas separation and gas exchange. In this study we designed, built, and operated a bioreactor that uses hydrophobic microporous membranes for gas exchange.

The membranes' oxygen gas flux and mass transfer coefficient (K_La) were characterized and compared using liquid flows of 2 liters per minute (LPM) and oxygen gas flows of 0.5 LPM. The highest observed oxygen flux during this test was 340 mg/(min*m²) for the flat sheet CLARCOR (QP952) membrane, and the highest rate of transfer, K_La , was 23.9 hr⁻¹ for the Liqui-Cel 2.5 x 8.0 hollow fiber module (X50 fibers, 1.4 m² membrane area). During tests and growth trials, water vapor diffused through the membrane pores into the gas channels and condensed, causing membrane wetting that impaired gas transfer by plugging pore spaces, which was mitigated by drying the membranes and membrane modules of any collected water. Bacteria slightly fouled the membranes during growth trials and reduced gas transfer. However, wetting impacted membrane gas transfer more than fouling during this study.

Bench-scale growth trials were inoculated with a consortium of type II methanotrophic bacteria dominated by the *Methylocystis* genus. Successful growth trials used parallel membrane module configuration. Growth trials that used the flat-sheet membrane QP952 and pure oxygen and methane gas streams produced bacteria with 22% PHB per dry cell mass. Growth trials using hollow fiber modules from Minntec (FiberFlo MCV-030) with mixed oxygen and methane streams produced bacteria with 46.9% PHB per dry cell mass. These results confirmed that membranes are capable of providing sufficient gas transfer for growth and production of PHB by methanotrophic bacteria.

TABLE OF CONTENTS

| | |
|--|-----|
| ABSTRACT | iii |
| LIST OF FIGURES | vii |
| LIST OF TABLES..... | x |
| ACKNOWLEDGEMENTS | xii |
| CHAPTER 1 INTRODUCTION | 1 |
| 1.1 Biopolymer and Methanotrophic Bacteria..... | 1 |
| 1.2 Global Warming and Plastic Pollution | 1 |
| 1.3 Industry Research Partnership | 2 |
| 1.4 Goals and Approach..... | 2 |
| CHAPTER 2 BACKGROUND INFORMATION | 3 |
| 2.1 Global Implications | 3 |
| 2.1.1 Greenhouse Gases in the Atmosphere | 3 |
| 2.1.2 Oceanic Pollution by Non-degradable Plastics..... | 4 |
| 2.2 Methanotrophic Bacteria..... | 5 |
| 2.2.1 Metabolism | 5 |
| 2.2.2 Cellular PHB Synthesis | 7 |
| 2.2.3 Characteristics and Uses of PHB | 7 |
| 2.3 Nitrogen Substrate and Methane Gas | 7 |
| 2.4 Membrane Gas Transfer | 8 |
| 2.4.1 Henry's Law and Gas Transfer..... | 9 |
| 2.4.2 Membranes..... | 11 |
| 2.4.3 Previous Membrane Characterization | 11 |
| CHAPTER 3 MATERIALS AND METHODS | 14 |
| 3.1 Membrane-Based Bioreactor Design | 14 |
| 3.1.1 System Design | 14 |
| 3.1.2 Initial Membrane Selection | 16 |
| 3.1.3 Flat Sheet and Hollow Fiber Membrane Modules | 17 |
| 3.1.4 Material Compatibility with Methane and Oxygen | 17 |

| | | |
|-----------|--|----|
| 3.2 | Gas Transfer Testing..... | 19 |
| 3.2.1 | Oxygen Gas Transfer Testing Procedure..... | 19 |
| 3.2.2 | Oxygen Gas Stripping Testing Procedure..... | 20 |
| 3.2.3 | Determination of K_La and Membrane Flux..... | 20 |
| 3.3 | Growth Medium..... | 21 |
| 3.4 | Methanotrophic Culture Microcosms..... | 21 |
| 3.5 | Growth Trial Operation..... | 22 |
| 3.5.1 | Pure Gas and Gas Mixture Operation..... | 22 |
| 3.5.2 | Liquid Flow Rate Alterations..... | 23 |
| 3.5.3 | Module Draining..... | 23 |
| 3.6 | Measurement Methods..... | 23 |
| 3.6.1 | Microbial Growth Measurements..... | 23 |
| 3.6.2 | Ammonium and Nitrate Consumption..... | 24 |
| 3.6.3 | PHB Confirmation Testing..... | 24 |
| 3.7 | Sources of Error..... | 25 |
| 3.7.1 | Manual Control Methods..... | 25 |
| 3.7.2 | Methane Measurements..... | 25 |
| 3.7.3 | Bacterial Growth Measurements..... | 25 |
| 3.7.4 | PHB Confirmation Testing..... | 26 |
| CHAPTER 4 | RESULTS AND DISCUSSION..... | 27 |
| 4.1 | Membrane Gas Transfer Results..... | 27 |
| 4.1.1 | Operational Changes..... | 29 |
| 4.1.2 | Hydraulic Pressure on the Membrane, Wetting, and Fouling..... | 32 |
| 4.1.3 | Growth Trial with Pure Gases and Flat Sheet Modules in Series..... | 33 |
| 4.2 | Growth Trial with Pure Gases and Flat Sheet Modules in Parallel..... | 36 |
| 4.2.1 | PHB Trial without Nitrogen Consumption..... | 37 |
| 4.3 | Growth Trials with Gas Mixture and Flat Sheet Membrane..... | 38 |
| 4.4 | Growth Trials with Gas Mixture and Hollow Fiber Membrane..... | 40 |
| 4.5 | Discussion of Growth Trials..... | 42 |

| | |
|--|----|
| CHAPTER 5 CONCLUSIONS | 44 |
| 5.1 Investigation Summary | 44 |
| 5.2 Recommendations for Further Research | 45 |
| REFERENCES CITED..... | 47 |
| APPENDIX A | 51 |
| APPENDIX B | 52 |
| APPENDIX C | 53 |
| APPENDIX D | 54 |

LIST OF FIGURES

| | | |
|------------|--|----|
| Figure 2-1 | A simple version of the serine cycle molecular pathway used by methanotrophic bacteria. Acronyms for major enzymes are in green. Abbreviations: MMO, methane monooxygenase; MDH, methanol dehydrogenase; H ₄ MPTP, methylene tetrahydromethanopterin pathway; MtdA, methylene tetrahydromethanopterin dehydrogenase; FDH, formate dehydrogenase; STHM, serine hydroxymethyl transferase; HPR, hydroxypyruvate reductase; MD: malate dehydrogenase; MTK, malate thiokinase; MCL, malyl coenzyme A lyase (Fei, 2014). | 6 |
| Figure 2-2 | Thin film model for the membrane contactor. Dashed lines indicate where molecular transport is driven by diffusion, and solid lines indicate where mixing drives molecular transport. The large arrow on the right indicates the diffusion of methane and oxygen from the gas phase into the liquid phase, but transport of water vapor and carbon dioxide from bacterial respiration also occurs in the reverse direction. This figure was adapted from Hemond & Fechner (2015). | 9 |
| Figure 2-3 | Left: Comparison of vapor flux across the 17 membranes used for MD; system operated with the feed stream 40 °C warmer than the distillate stream, 1.6 LPM countercurrent flow rates, and 1 g/L NaCl in the feed solution. Right: Contact angle comparison for the same 17 membranes (Vanneste et al., 2017). Error bars on average water flux and membrane contact angle graphs represent the standard deviation of four measurements and ten measurements, respectively..... | 13 |
| Figure 3-1 | Bioreactor configuration with membrane modules operating in parallel in separate loops. Each module delivers a pure gas, and gas streams do not mix..... | 15 |
| Figure 3-2 | Bioreactor configuration with membrane modules operating in series in the same loop. Either methane or oxygen is delivered and exhausted to the atmosphere in each membrane module to prevent mixing of gases. In this drawing the methane is delivered first, but the operation was also reversed to deliver oxygen first..... | 16 |
| Figure 3-3 | Flat-sheet and Minntec hollow fiber module. Flat sheet module dimensions are 16 inches by 6 inches, but surface area of the hollow fiber module is a factor of 10 higher.. | 18 |
| Figure 3-4 | Gas transfer test results for a HF and FS module. | 21 |
| Figure 4-1 | Comparison of membrane gas flux; FS represented as solid bars, and HF as hatched bars. Oxygen flux was calculated in the concentration range from 2 to 4 mg/L DO. Tests were performed with liquid flow rate of 2.0 LPM, and gas flow rates of 0.5 LPM. Error bars represent standard deviation based on three tests under the same conditions..... | 27 |
| Figure 4-2 | K _L a values calculated for membranes: FS are solid bars, and HF are hatched bars. Testing was performed with liquid flow rate of 2.0 LPM, and gas flow rates of 0.5 LPM. The K _L a value was obtained from data within 2-4 mg/L. Error bars represent standard deviations based on three tests under the same conditions. | 29 |
| Figure 4-3 | Comparison of packing density for the HF modules used in this study (hatched bars) and a FS spiral wound module (dotted bar). Columns indicate the packing density, and the red diamond points indicate the total surface area of each module..... | 30 |
| Figure 4-4 | Gas exchange of CLARCOR QP952 at different liquid flow rates; gas flow rate was set to 0.5 LPM for all tests. Standard deviation is represented by error bars, and was calculated from three tests..... | 30 |

| | | |
|-------------|---|----|
| Figure 4-5 | Flux comparison of HF membrane at various liquid flow rates; gas flow rate was set to 0.5 LPM. Filled data points represent conditions with gas at atmospheric pressure during operation. Hatched points and dotted points were obtained while pressurizing the oxygen gas at 10 psig and 15 psig, respectively, in the module during testing by restricting flow at the outlet of the HF module..... | 31 |
| Figure 4-6 | $K_L a$ calculated for HF membranes at different liquid flow rates and 0.5 LPM of oxygen. Filled data points represent conditions with gas at atmospheric pressure during operation. Hatched points and dotted points were obtained while pressurizing the oxygen gas at 10 psig and 15 psig, respectively, in the module during testing by restricting flow at the outlet of the HF module..... | 32 |
| Figure 4-7 | Liquid pressures generated by increased flow rates in HF modules. Manufacturer-recommended operational pressure is below 30 psig except for PermSelect, for which less than 45 psig is recommended. | 33 |
| Figure 4-8 | Oxygen flux results from CLARCOR QP952 testing under different membrane states. Oxygen flow rate was 0.5 LPM, and liquid flow rate was 2.5 LPM. Fouled membranes were used in growth trials operating with mixed or pure gases prior to gas exchange testing; pure gas operation fouled the methane module..... | 34 |
| Figure 4-9 | A compilation of three bacteria growth trials, where modules were used in series, and PHB was never produced. Circles (growth trial 1) represent measurements using a 20 mL Hach vial and triangles (growth trials 2 and 3) represent OD measurements using a 200- μ L quartz cuvette. | 35 |
| Figure 4-10 | Results of effective oxygen flux tests for CLARCOR QP952 membrane used in series and parallel operation with pure oxygen and pure methane in separate modules. Order of gases is denoted on the x-axis. Parallel configuration has modules in separate loops. Calculations used a DO range of 2-4 mg/L. | 35 |
| Figure 4-11 | Microbial growth measured as OD during a growth trial using pure gases with flat sheet modules in parallel. DO is the dark blue line. Ammonium and nitrate were depleted at 100 hours and is indicated by a red line..... | 36 |
| Figure 4-12 | Consumption of nitrate and ammonium, and bleach ratio tests performed during the growth trial using pure gases with flat sheet parallel modules. At 100 hours, nitrogen sources are depleted, and PHB production begins..... | 37 |
| Figure 4-13 | Microbial growth measured as OD and PHB production measured by FTIR during a growth trial using pure gases with flat sheet modules in parallel. DO is the dark blue line. Nitrogen sources were absent during this trial, and bacteria were previously grown at Mango Materials..... | 38 |
| Figure 4-14 | Optical density and oxygen concentrations of a growth trial using flat sheet membrane QP952 and a 1:1 methane oxygen gas mixture by volume, in two separate modules, in parallel configuration. Flow rates of both liquid loops were 2.0 LPM. The red line indicates ammonium and nitrate depletion, where PHB production began. | 39 |
| Figure 4-15 | Consumption of nitrogen sources by bacteria, and bleach ratio tests for PHB production, in flat sheet QP952 mixed gas growth trial. PHB mode started at ~75 hours..... | 40 |
| Figure 4-16 | Optical density and DO during the growth trial using two Minntec MCV-030 HF modules (0.2323 m ²) with mixed gases. The red line indicates ammonium and nitrate | |

depletion, where PHB production began. DO was depleted after 20 hours due to a conservative gas mixture composition, which was subsequently increased to 1:1 parts methane to oxygen.41

Figure 4-17 Ammonium and nitrate consumption and bleach ratio tests for PHB production, in hollow fiber mixed gas growth trial. PHB production began at ~40 hours. Increased bleach dilutions were used at the end of this trial to compensate for the denser culture produced in this trial.41

Figure A-1 Membrane-based bioreactor operating with two flat-sheet modules during a growth trial.51

Figure B-1 Gas transfer testing using hollow fiber module from Minntec. Liquid was either passed through the lumen (circles) or the shell (triangle) using different liquid flow rates.52

Figure C-1 K_La (left) and flux (right) for FS QP952 under different oxygen gas and liquid flow rates; temperature was maintained at 30 °C. Error bars represent standard deviation based on three tests.53

Figure D-1 Optical density and VSS measurements are correlated. Graph on the left uses the entire data set and uses a logarithmic trend; graph on the right uses data that appeared linear and uses a linear trend. The bacterial culture was obtained from the growth trial that used hollow fiber modules and gas mixture. Samples were diluted to different ODs and filtered afterwards. Error bars represent the standard deviation of three samples.54

LIST OF TABLES

| | | |
|-----------|--|----|
| Table 2-1 | Characteristics of gas transfer membranes (Vanneste et al., 2017). For this study, CLARCOR QL822, CLARCOR QP952, and 3M 0.45 μm were used. | 12 |
| Table 3-1 | Characteristics of flat-sheet membranes used for testing in this study. Data for the FS membrane are from (Vanneste et al., 2017) | 17 |
| Table 4-1 | Comparison of Growth Trial Performance | 42 |

LIST OF ACRONYMS

| | |
|-------|---|
| ATP | Adenosine triphosphate |
| CSM | Colorado School of Mines |
| DDT | Dichlorodiphenyltrichloroethane |
| DI | Deionized |
| DO | Dissolved oxygen |
| ECTFE | Ethylene chlorotrifluoroethylene |
| FS | Flat-sheet |
| FTIR | Fourier transform infrared spectroscopy |
| GC | Gas chromatography |
| HA | Hydroxyapatite |
| HF | Hollow fiber |
| LEPW | Liquid entry pressure of water |
| LMH | Liters per meter squared per hour |
| LPM | Liters per minute |
| MD | Membrane distillation |
| MM | Mango Materials |
| NADH | Nicotinamide adenine dinucleotide hydride |
| NASA | National Aeronautics and Space Administration |
| NPSG | North Pacific Subtropical Gyre |
| OD | Optical density |
| ODO | Optical dissolved oxygen |
| PAH | Polyaromatic hydrocarbon |
| PCB | Polychlorinated Bisphenol |
| PE | Polyethylene |
| PEP | Phosphoenolpyruvate |
| PHA | Polyhydroxyalkanoate |
| PHB | Polyhydroxybutyrate |
| PP | Polypropylene |
| PTFE | Polytetrafluoroethylene |
| PVDF | Polyvinylidene difluoride |

ACKNOWLEDGEMENTS

I owe a debt of gratitude to a great many people who during every single step of this project gave me support, assistance, guidance, a boot at the right moment, inspiration, and knowledge. First and foremost, thank you Professor Junko Munakata Marr, for not only creating this opportunity through your partnership with Mango Materials, but especially for deciding to have me work on this project with you as a graduate student. I sincerely appreciate the opportunity and all the guidance, support, time, late night editing, energy, and encouragement you have given me over the last year; without you I would probably still be in Hawaii instead of having progressed my education and experience in amazing ways. Thank you Professor Tzahi Cath, you not only started me down the road of using and understanding membranes, but have challenged me to think like a researcher, and get out there to show it to other researchers. You told me that I needed to leave my mark on research, and with your guidance I hope that this is exactly what we have done. I greatly appreciate all your support throughout this, albeit sometimes painful, process, and the extra rabbit holes we went down during my time here at CSM. As my advisors, I have the utmost respect and appreciation for you both.

Mike Veres, you have helped me improve my common sense at least an order of magnitude, and kept me in check while playing with explosive gases. Thank you most for your enthusiasm for this project and helping me work out ideas on the fly, and for listening to my often-wild ideas. Johan Vanneste, without you, there would be no K_L club, and I would not fully understand how to describe gas transfer with membranes as well as I do now; your waffles kept me going. Dr. Linda Figueroa, you have helped me understand not only how to think about microbial growth, but how to describe it; without that help, there would be no modeling chapter in this thesis. Dr. John Spear, from reading between the lines to meat composting, and enlightening me on the amazing contributions from the microbial community to our world, you inspired me to dig further into what is happening and always ask the question “who is there?” I want to thank Mango Materials, Allison Pieja, and Joe Lampe, for their contributions to my understanding of how this culture functions, where to start on this project, and the use of their ODO probe for an extended period of time. Being able to see both sides of this research and tie things together in my minds has truly inspired me. This project would not have been possible without all of that help, and I sincerely thank you all, you were each critical to the success of this study.

This project, and my time as a graduate student was funded in part by NASA, and made this possible for me. Thank you also to the Sussman Foundation for funding my internship at Mango Materials, and giving me the time I needed over the summer to complete the research and writing. I also want to acknowledge the opportunities given to me by my advisors to ensure we were able to keep my funding going, especially because of the fun side projects we were able to do.

Last but certainly not least, thank you to my family and my friends for always being a constant source of support when I needed it most. You helped me put myself back together, and always encouraged me to keep going forward and not give up when work became overwhelming.

CHAPTER 1 INTRODUCTION

Both non-degradable plastic pollution and global warming due to increasing concentrations of greenhouse gases are major global problems. Methane is a potent greenhouse gas that some bacteria, known as methanotrophs, consume as a carbon and energy source. Specific types of methanotrophs can store methane as intracellular polymer in response to nitrogen-deficient conditions. This chapter first introduces the pertinent bacteria, the environmental relevance of the biological process, the organizations involved in this research, and the goals of this study.

1.1 Biopolymer and Methanotrophic Bacteria

Biologically produced polyhydroxyalkanoate (PHA) has been investigated over the years as a useful biopolymer. Polyhydroxybutyrate (PHB) is a specific PHA polymer that type II methanotrophic bacteria accumulate as cellular inclusions during macronutrient limitations such as the absence of viable nitrogen sources. PHB inclusions are these bacteria's carbon storage mechanism, and PHB is then used once nitrogen becomes available. This presents a potentially viable method of producing the biopolymer PHB, which is a polyester that exhibits thermoplastic behavior similar to polypropylene, is biodegradable and biocompatible, and may be used as a replacement for synthetic polymers (Lichtenthaler, 2010).

1.2 Global Warming and Plastic Pollution

Bacterial production of PHB using otherwise wasted methane gas as feedstock can contribute to the reduction of methane gas emissions to the atmosphere. Both methane and CO₂ are greenhouse gases because they absorb energy from infrared radiation, but methane is more potent. Reduction of methane emissions helps to reduce the impacts of global warming, and methanotrophic bacteria consume this gas. In the absence of nitrogen, bacteria produce PHB, which is a biodegradable polymer that is less persistent than petroleum based products in the environment (Doi et al., 1992).

Petroleum-derived plastics have gained attention as a global problem due to their collection in oceanic gyres; a total of eleven gyres are scattered throughout the oceans. Concentration estimates in the North Pacific subtropical gyre (NPSG) based on surface trawling averaged 334,271 pieces or 5,114 g per km² (Moore et al., 2001). A more recent study by the same team, using drones to aerially view the surface of the ocean, indicates that the concentrations are likely two orders of magnitude higher than previously thought (Evers, 2014). The area of the NPSG is 20 million km²; therefore, the total mass of plastic in the NPSG is immense. The majority of this plastic is petroleum-based and may require more than a century to completely degrade (Siddique et al., 2008). Studies have shown that the presence of plastics in marine environments allows chemical transport into the food chain due to the affinity of compounds like DDT and PCB to adsorb to their surfaces (Beaman et al., 2016; Derraik, 2002; Eriksen et al., 2017). Sorption occurs over time; thus, the reduction of plastic's residence time in marine

environments equates to a reduction in plastic's contact with chemicals (Engler, 2012). This in turn may reduce the concentrations being introduced to the food chain when plastics are mistaken for food by marine life (Engler, 2012). PHB and other biodegradable polymers are potentially less persistent in the environment, and PHB produced by bacteria may prove to be a solution to environmentally persistent plastics.

1.3 Industry Research Partnership

Mango Materials (MM) is a start-up company based in Albany, CA. Their bioreactor systems produce PHB from local waste methane sources using a direct gas sparging system, and have the goal of being economically competitive with petroleum-derived polymers (Mango Materials, 2011). MM is working toward commercializing biological reactors that deliver dissolved gases to methanotrophic bacteria capable of synthesizing PHB (Mango Materials, 2016). Colorado School of Mines (CSM) and MM began collaborating based on complementary expertise in membranes and biological reactors. A successful joint proposal submission for Phase I funding to the National Aeronautics and Space Administration (NASA) supported CSM and MM to prototype a novel membrane-based biological reactor. The long-term goal is to develop an efficient system for production of PHB that does not depend on gas sparging in the bioreactor, enabling operation in microgravity environments, a specific interest of NASA.

1.4 Goals and Approach

The goal of this study was to use membranes for gas transfer in a bioreactor capable of producing bacteria with PHB inclusions as proof-of-concept for the NASA Phase-I project. NASA is interested in microgravity operations, which presents a specific challenge: in microgravity, bubbles do not exit liquid solutions because of the lack of buoyant forces created by gravity. If methane and oxygen gas bubbles collect, their mixture is a safety concern. Membranes can separate the gases and liquid medium, addressing safety with respect to uncontrolled gas mixtures while also facilitating enough contact between gases and liquid medium for the gases to dissolve and feed bacteria growth.

We specifically investigated membrane contactors using hydrophobic microporous membranes to determine if gas transfer was sufficient for bacteria growth and PHB production. Gas transfer performance of membranes was characterized during this study by flux and gas transfer rate (K_La). This information was used to determine which flat-sheet and hollow fiber membranes would be used during growth trials in the bioreactor. Experiments were conducted with membrane modules configured in series and in parallel to determine if either configuration was more advantageous for bacterial growth. Pure gases and gas mixtures were used with the same goals in mind. The successes and failures associated with these experiments provided insight into challenges the project will face.

CHAPTER 2

BACKGROUND INFORMATION

The main objective of this study was to determine whether a membrane-based bioreactor could provide type II methanotrophic bacteria with sufficient dissolved oxygen and methane for growth and production of polyhydroxybutyrate (PHB). The use of membranes to deliver dissolved gases to bacteria was the defining difference from gas sparging systems. Efficient bioreactors of either gas-delivery format that ultimately yield PHB are important developments and have global implications. This chapter begins with the current impacts of methane and petroleum-based plastics on a global level, proceeds to describe the bacteria that produce PHB, introducing valuable properties of PHB, discusses gas exchange, and ends with information on the membrane types investigated for this application.

2.1 Global Implications

Global plastic pollution has resulted from poor waste management allowing environmentally resistant plastics to enter various environments such as the ocean. Biodegradable products could be a solution to this, and bacterially sourced PHB is a polymer proven to degrade in wastewater (Gulliver, 2017). Microbes possessing enzymes that can degrade PHB are also ubiquitous in the environment (Holmes, 2002). Methane, this study's primary feedstock for production of PHB by methanotrophic bacteria, is a potent greenhouse gas. Methane is considered a significant contributor to atmospheric greenhouse gases directly linked to climate change (Augenbraun et al., 2010; Rodhe, 1990). This section discusses how both bacterial consumption of methane and the use of biodegradable PHB may help address these global issues.

2.1.1 Greenhouse Gases in the Atmosphere

Methane gas is estimated to be responsible for 4-9% of the overall greenhouse effect, compared to carbon dioxide estimated at 9-26% (Randy, 2007). Global methane production, estimated at 500-520 Tg per year, is largely anthropogenic, with wetlands, methane hydrates, the ocean, and termites accounting for 29% of annual production (Augenbraun, 2010; Fung et al., 1991). Aerobic methane-oxidizing bacteria in various global environments annually consume an estimated 50% of all biologically produced methane, which does not account for anthropogenic sources (Ho et al., 2013; Conrad, 2009). Methane in the atmosphere is also involved in photochemical reactions that can produce ozone, carbon dioxide, and water vapor, all of which are greenhouse gases (Henning, 1990). Thus, when bacteria consume methane, they decrease the potential of photochemical formation of other greenhouse gases in the atmosphere, and reduce the amount of methane entering the atmosphere.

Commercial and industrial processes require energy inputs that are often derived from fossil fuel combustion, which produces the greenhouse gas CO₂. Methane combustion also produces CO₂, as does bacterial respiration. Processes and equipment that use fuels or electricity (i.e. pumps, heaters, cleaning,

transportation, etc.) to maintain the conditions required for bacterial growth either directly or indirectly produce CO₂. To determine if growth of methanotrophic bacteria reduces overall greenhouse gas emissions, the entire process needs to be considered in a life-cycle assessment, which is not currently available for a bacterial growth operation at the commercial-scale. A study of biotechnology's sustainability, versus using conventional methods of polymer production, indicated greenhouse gas emissions vary depending on how the required substrate was produced, whether the transportation of the substrate was considered, and the operation of the process itself (Gerngross, 1999). One advantage of operating a reactor at a wastewater plant is that the substrate transportation is minimal, because the waste stream can be used to produce substrate for bacteria growth. Corn is sometimes used to produce a methanol substrate, in contrast to wastewater or waste stream organics. A study investigating organics reclaimed from a landfill waste stream found that the organics were more favorable with respect to the inputs required for bacteria growth when compared to methanol production from corn, which requires more fossil fuels to produce (Harding et al., 2007). Further study of different bioreactors and associated processes is needed to make any solid claims to being sustainable or having lower greenhouse gas emissions, but methanotrophic bacteria do uniquely use methane gas sources, which presents a new avenue of use beyond combustion for heating or flaring.

2.1.2 Oceanic Pollution by Non-degradable Plastics

The North Pacific subtropical gyre, a massive spinning whirlpool powering the oceanic current, is currently teeming with plastic, and is one of eleven gyres present in the oceans around the world. Plastic debris concentrations were estimated to be 5.114 kg/km² in the North Pacific Subtropical Gyre in 2001 (Moore et al., 2001). That mass estimate only included oceanic plastic from the ocean's surface where trawling and visual confirmation occurred; recent aerial observations indicated that this mass is likely much higher (Evers, 2014). Since estimates do not include any sunken or suspended plastic debris, the next mission of the Algalita Marine Research Foundation is the characterization of plastic masses within the water column to increase the accuracy of debris estimates. All of this pollution results from conventional materials produced with petro-chemicals that are designed to be environmentally resistant.

The advantage of using PHB is that it is 100% biodegradable, and presents a partial solution with respect to plastics that do not degrade well after entering the environment (Getachew & Woldesenbet, 2016). The time required for degradation of PHB ranges from months in anaerobic sewage to years in seawater (Madison & Huisman, 1999). Many species of bacteria in soil and marine environments are able to make PHA hydrolases and depolymerases responsible for PHA degradation (Jendrossek et al., 1996). In comparison, petrochemical based products are intentionally designed to be resistant to degradation, and are estimated to persist in the environment for centuries depending on the thickness and type of plastic (EPA, 2016).

Plastic debris is mistaken for food by marine life, and it is well documented that turtles mistake plastic bags as jellyfish, guts of deceased avian species are often filled with plastic pieces, and fish ingest

small plastic pieces (Beaman et al., 2016; Moore et al., 2001). Plastic in the ocean is exposed to weathering from physical and chemical processes that include exposure to ultraviolet light, waves, and the wind. Over time, this breaks down larger plastic pieces into smaller bits and causes cracks and changes to the material that likely increase the surface area. Chemicals such as dichlorodiphenyltrichloroethane (DDT), polychlorinated bisphenols (PCBs), polyaromatic hydrocarbons (PAHs), and metals are all present in the ocean due to human activities (Beaman et al., 2016; Teuten et al., 2009). These chemicals are adsorbed by plastics because hydrophobic compounds such as PCBs and PAHs have an affinity for plastics (Engler, 2012). Therefore, marine life ingests not only plastics, but the chemicals adsorbed to them. As fish and other marine life consume plastics and are then consumed by organisms higher on the food chain, the chemicals bioaccumulate in increasing concentrations at higher trophic levels of the ecosystem. Ultimately, all different levels of the food chain have toxic chemicals in their biology due to plastic consumption, and humans are at the top, consuming marine life that has been biologically accumulating toxins from the environment over time.

2.2 Methanotrophic Bacteria

Large volumes of methane gas are produced globally every year. In the early 19th century, Söhngen (1906) suggested that atmospheric concentrations were lower than expected because of microbial oxidation, and he subsequently isolated several species, including the first known methanotroph, *Bacillus methanicus*. Methane-oxidizing bacteria require methane, oxygen, and nitrogen for their metabolism and cell synthesis, and are a diverse group responsible for the mitigation of atmospheric methane.

Type II methanotrophs are α -proteobacteria, and include the genus *Methylocystis*. These organisms have a k-type life strategy, meaning that their use of available energy emphasizes characteristics associated with survival and longevity instead of rapidly reproducing (Golovlev, 2001). This life strategy is contrasted by the r-type life strategy of heavily investing energy into reproduction, which is exhibited by type I methanotrophs. Due to this difference in life strategy, type I outcompetes the type II when environmental conditions are favorable for growth, but in dry conditions and cold conditions, the type II methanotrophs continue oxidizing methane while the type I methanotrophs do not (Siljanen et al., 2012).

2.2.1 Metabolism

Type II methanotrophs are considered obligate methanotrophs because they are unable to utilize any known gluconeogenic pathways involving pyruvate and acetate (Shishkina & Trotsenko, 1982). Acetyl-CoA cannot play an important role in pyruvate metabolism due to the low activity of pyruvate dehydrogenase within the pyruvate dehydrogenase complex (Shishkina & Trotsenko, 1982). Lack of enzymes phosphoenolpyruvate (PEP) synthetase and pyruvate phosphate dikinase also prevents the synthesis of PEP. Metabolic pathways such as the Krebs cycle are not viable for these bacteria because

isocitrate lyase and malate synthase enzymes responsible for replenishing cycle intermediates are not present (Shishkina & Trotsenko, 1982).

These bacteria are capable of using particulate or soluble methane monooxygenase to convert methane into methanol, and then to formaldehyde using methanol dehydrogenase (Anthony, 1986). Carbon dioxide, adenosine triphosphate (ATP), and nicotinamide adenine dinucleotide hydride (NADH) are used to convert formaldehyde into the 2-phosphoglycerate used to generate cellular material according to the stoichiometric Equation 2.1 (Hanson & Hanson, 1996):



Formaldehyde is transformed via the methylene tetrahydromethanopterin pathway to formic acid, which is transformed to $\text{CH}_2=\text{H}_4\text{F}$ using methylene tetrahydromethanopterin dehydrogenase, and is converted to serine to be used according to the cycle in Figure 2-1 (Hanson & Hanson, 1996). A product of the serine cycle is acetyl-CoA, which can generate energy within the incomplete Krebs cycle and is used to produce PHB (Hanson & Hanson, 1996; Shishkina & Trotsenko, 1981).

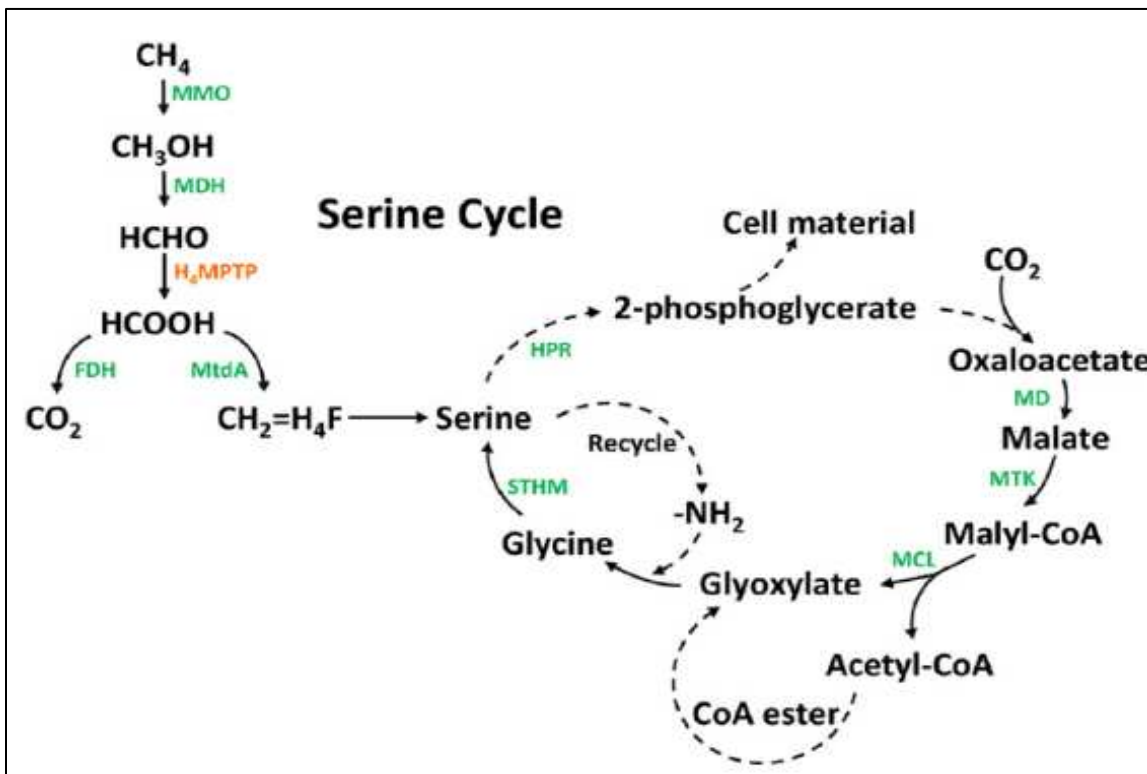


Figure 2-1. A simple version of the serine cycle molecular pathway used by methanotrophic bacteria. Acronyms for major enzymes are in green. Abbreviations: MMO, methane monooxygenase; MDH, methanol dehydrogenase; H₄MPTP, methylene tetrahydromethanopterin pathway; MtdA, methylene tetrahydromethanopterin dehydrogenase; FDH, formate dehydrogenase; STHM, serine hydroxymethyl transferase; HPR, hydroxypyruvate reductase; MD: malate dehydrogenase; MTK, malate thiokinase; MCL, malyl coenzyme A lyase (Fei, 2014).

2.2.2 Cellular PHB Synthesis

Two molecules of acetyl-CoA, formed by the serine cycle, are condensed into acetoacetyl-CoA, which is reduced to form the hydroxybutyryl-CoA that can be polymerized into PHB (Uchine et al., 2007). This polymer may be hydrolyzed to form 3-hydroxybutyrate, a different form of PHB. Intracellular PHB granules only remain while nitrogen sources are not present, and are consumed once nitrogen sources are available. Thus, the collection of intracellular masses of PHB depends on sustaining nitrogen-depleted environments while bacteria are being grown.

2.2.3 Characteristics and Uses of PHB

PHB has similar properties to polypropylene with respect to melting temperature, glass transition temperature, crystallinity, and tensile strength (Dobroth et al., 2011). Longer polymer chains are more valuable for commercial purposes, and are reflected as higher molecular weight. Applications for PHB include reinforcement for natural fiber composites, cosmetics, *in vivo* or *in vitro* medical use, degradable packaging, and generally as a plastic alternative (Chen et al., 2000; Tayton et al., 1982; Dobroth et al., 2011). Studies on surgical implants report that combinations of hydroxyapatite (HA) with PHB can be used as a material that can be injection molded and may be a replacement for stainless steel for orthopedic implants, or as a graft material that stimulates localized bone formation (Tanner, 2010; Boeree et al., 1993; Coats et al., 2008; Tayton et al., 1982). The desired effect of using a PHB/HA mix is that both are bioactive materials, which the human body can interact with on a cellular level, allow better bonding between implants and tissues, and lead to a decreased risk of long-term rejection and infection (Tanner, 2010). More investigation of these applications for PHB with other copolymers is needed to generate a material with qualities comparable to stainless steel, but its biocompatible nature as a material is very promising.

2.3 Nitrogen Substrate and Methane Gas

Studies performed with other bacteria that produce PHAs using substrates such as crude glycerol, olive oil mill waste streams, propionate, or glucose indicated that the composition of the substrate impacts the quantity and quality of the end product (Dobroth et al., 2011; Koutinas et al., 2007). One study investigated the use of glyoxylate, an intermediate of the serine cycle, to determine its impacts on methanotrophic growth and found that glyoxylate was not readily consumed during culture growth with methane and nitrogen (Pieja et al., 2011). Another study used ammonium, nitrate, and nitrogen gas as substrates for methanotrophic growth and found that PHB production ranged from 11% to 46% (based on dry cell mass) depending on the species and which nitrogen source was used (Rostkowski et al., 2013).

Methane must be provided to feed methanotrophic bacteria that produce PHB. Sources such as “natural gas” or “biogas” are available resources produced by human activities, including petroleum reservoirs, landfills, anaerobic digesters at wastewater treatment plants, and biogas production plants. A primary consideration for these substrates is whether the gas composition is appropriate for bacteria to

produce PHB. If the gas source being used contains other gases, then the partial pressure of methane in the gas mixture is reduced, and this reduces the concentration in solution; this is further discussed in the next section.

Gases produced by the aforementioned processes are often flared because the gases are not pure enough to comply with standards for public distribution networks, but are also flared when production is too high for gases to be completely captured (EPA, 2017). Global production of natural gas from wells in 2012 resulted in flaring, estimated via satellite, of 143 billion cubic meters of methane (Tollefson, n.d.). Flaring occurs at landfills, where methane is produced by methanogenic bacteria under anaerobic conditions from deposited solid waste (EPA, 2017). Anaerobic digesters produce biogases comprised of methane (57–66%), carbon dioxide (33–39%), nitrogen (1–10%), and oxygen (<0.5%), and trace amounts of chlorides, hydrogen sulfide, and ammonia (Amon et al., 2007; Boyle, 1976; Spiegel & Preston, 2000). Regulations associated with distribution of renewable natural gas, or biogas, produced by anaerobic digesters include the removal of CO₂, H₂S, and moisture (Litter, 2012). According to the composition of biogases from Spiegel & Preston (2000), regulated gas qualities of approximately 90% methane, with minor impurities, would be available to produce PHB with methanotrophic bacteria. Mango Materials currently uses such a biogas from a wastewater treatment plant, and successfully grows methanotrophic bacteria that produces PHB (Mango Materials, 2016).

Methane gas can also be produced at specific biogas plants using different organic inputs. Processes may utilize corn, wheat, or even algae to produce methane biogas via digesters (Amon et al., 2007; Dębowski et al., 2013). Another study reported that crop yields per hectare of land peaked at 27,500 kg of maize, which was used to produce about 6000 m³ of methane (Amon et al., 2007). These numbers equate to the production of 21.8 dm³ of methane per kg of maize used as digester substrate. Another study explored using algae as biomass for use in digesters, using wastewater to grow the algae, and resulted in biogas production ranging from 150 dm³/kg to 986 dm³/kg of biomass (Dębowski et al., 2013). Algae appear to be more productive on a mass-to-mass basis, and would not interfere with production of food crops. Algae can also be grown at a wastewater facility and contribute to nutrient removal (Dębowski et al., 2013).

2.4 Membrane Gas Transfer

The system prototyped during this study can be described using a thin film model where liquid medium makes contact with the membrane, specifically the pore spaces of the membrane, at the gas-liquid interface. The thin film on the gas side is the membrane, where gas transport in the pore space is governed by diffusion, and the thickness of the film is the thickness of the membrane. On the liquid side of the membrane is a thin film of medium that is assumed to be in equilibrium (saturated) with the gas phase at the interface, and transport away from the interface is governed by diffusion from the interface through the thin film to the bulk liquid (Hemond & Fechner, 2015). Transport of gas in the thin film into the bulk medium flowing across the membrane results in overall mass transport of gases into the bulk

medium where bacteria grow. This system of interfaces is depicted in Figure 2-2.

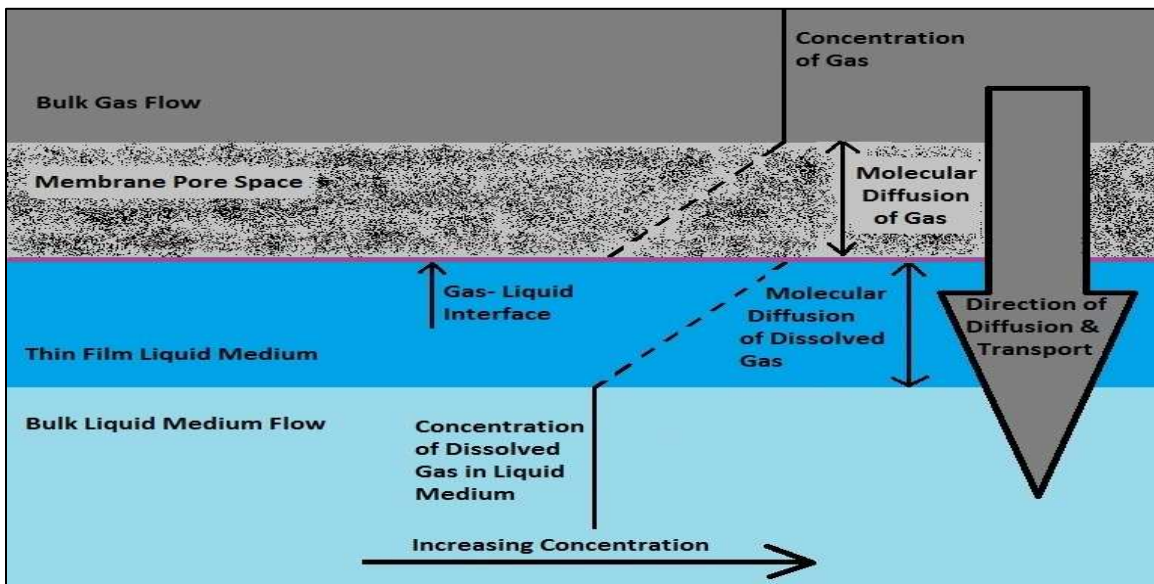


Figure 2-2. Thin film model for the membrane contactor. Dashed lines indicate where molecular transport is driven by diffusion, and solid lines indicate where mixing drives molecular transport. The large arrow on the right indicates the diffusion of methane and oxygen from the gas phase into the liquid phase, but transport of water vapor and carbon dioxide from bacterial respiration also occurs in the reverse direction. This figure was adapted from Hemond & Fechner (2015).

The concentration of dissolved gas in the medium at the interface is assumed to be at equilibrium, as defined by Henry's Law (Equation 2.2). Once gases are dissolved, the bacteria can use them for growth and PHB production. Currently, Mango Materials uses direct gas sparging for gas delivery to the methanotrophs, and calculates their system's gas exchange using the mass transfer parameter $K_L a$. To compare our results in terms of exchange rate, $K_L a$ was calculated for the membranes used. Flux was also calculated in this study to directly compare how well the membranes performed gas transfer based on area; flux will be useful for future studies to determine the required membrane area for sufficient transfer of oxygen and methane.

2.4.1 Henry's Law and Gas Transfer

Henry's Law describes the equilibrium point between gas phase partial pressure and the gas concentration dissolved in the liquid phase. The concentration of the gas in solution is directly related to the partial pressure of the gas in the headspace, or in this case the gas stream on the other side of the membrane. This relationship is defined according to Equation 2.2, where $k_{H,cp}$ is Henry's constant in units of atm/M, C_{sat} is the equilibrium or saturation concentration of dissolved gas in the liquid in mol/L or M, and P is the partial pressure of the gas stream in atm.

$$k_{H,cp} = \frac{P}{C_{sat}} \quad (2.2)$$

Literature reports values for Henry's constant for methane and oxygen of 704.95 and 769.23 M/atm, respectively (Sander, 2015). The saturation concentration of the gases dissolved into the liquid can be found using these values and atmospheric pressure. The laboratory where this study was conducted is at 6000 ft above sea level, and the average atmospheric pressure is approximately 0.803 atm (Engineering Toolbox, 2017). Based on 0.803 atm and the Henry's constants, the concentrations of methane and oxygen at saturation are 1.139×10^{-3} and 1.044×10^{-3} M (18.2 and 33.4 mg/L), respectively, for pure gas in equilibrium with water.

Henry's Law does not describe how quickly gases diffuse into solution, but this can be determined by measuring the change in concentration of dissolved gas in solution. The transfer of gases into solution is controlled by two variables: concentration difference of dissolved gas in solution from the saturation concentration, and the area available for transfer to occur (Kreulen et al., 1993). $K_L a$ is the calculated mass transfer rate of a gas, where "a" is the area where gas makes contact with the liquid surface. $K_L a$ can be mathematically described (Equation 2.3) using saturation concentration for dissolved gas (C_{sat}), and the concentration in the liquid (C_w) (Chisti, 1989). Integration of Equation 2.3 yields Equation 2.4. When experimental trials are performed to determine $K_L a$, if the gas concentration being measured is initially zero or assumed to be zero, then C_0 can be neglected in Equation 2.4.

$$\frac{dC_w}{dt} = K_L a (C_{sat} - C_w) \quad (2.3)$$

$$\ln \left(\frac{C_{sat} - C_w}{C_{sat} - C_0} \right) = -K_L a t \quad (2.4)$$

The flux of gas relies on defining an area where mass transfer is occurring. The hollow fiber or flat-sheet membranes are the boundary where this occurs during our study. At the membrane, gases dissolve into solution where pore space is present for gases to make contact with the liquid; the rate of this phenomenon can be described using $K_L a$, which includes the mass transfer coefficient. Flux can be described using Equation 2.5, where $\frac{dC_w}{dt}$ is divided by the area of the membrane (Rishell et al., 2004).

$$Flux = \frac{K_L a (C_{sat} - C_w)}{Membrane\ area} \quad (2.5)$$

In Equations 2.3 through 2.5, mathematical variables define flux and K_L using the concentration difference $C_{sat} - C_w$. Thus, the mass transfer of gas into solution is the highest when concentration of dissolved gas is furthest from saturation and the difference is highest. As a usable metric to characterize membranes for future bioreactor design, an average membrane flux [$\text{mg}/(\text{min} \cdot \text{m}^2)$] was calculated in this study according to Equation 2.6, using liquid volume (V), and membrane area (A).

$$Flux = \frac{dC_w V}{dt A} \quad (2.6)$$

2.4.2 *Membranes*

Two types of membrane were used during this study: flat-sheet and hollow fiber. Both types of membrane facilitated gas transfer by diffusing gases into the membrane pore space, where gases make contact with and dissolve into the liquid. Previous studies indicate that to maintain membrane flux, pore space needs to be protected from being flooded (Cath et al., 2004; Nghiem & Cath, 2011). Liquid entry pressure of water (LEPW) is an important operational parameter that indicates the minimum pressure required for water to penetrate the membrane pore space. Flooded pore space reduces the area available for gas transfer, or generates membrane resistance due to a liquid barrier where gases dissolve in and out before reaching the bulk liquid.

Hydrophobic membranes were investigated in this study because hydrophobicity protects the pore space by repelling liquid water from the surface instead of allowing easy penetration. Contact angle is a measure of hydrophobicity that indicates how well the membrane repels water from its surface, and is directly related to how easily a surface will wet (Zheng & Lü, 2014). Liquid surface tension also keeps water out of the pore space while the liquid is not in direct contact with the hydrophobic membrane, but is over the pore space. A small pore size allows the surface tension to protect the membrane pore space; a larger pore size requires less force for water to enter the pore space.

During operation with liquid and gas on opposing sides of the membrane, water vapor also crosses the membrane and condenses on the gas side of the membrane. If water condenses inside the pore space, it creates a barrier to gas transfer through the pores. When water contacts the gas side of the membrane, it also creates a barrier for gas transfer.

2.4.3 *Previous Membrane Characterization*

Membrane characteristics that are relevant for this study include vapor flux, contact angle, nominal pore size, thickness, and porosity. Vapor flux is the volume of liquid water that passes through the membrane as water vapor, and is reported as liters per meter squared per hour (LMH); the transport of methane and oxygen is synonymous because they follow the same paths through the membrane pore space. Gases may pass through the pore space of a membrane to contact and dissolve into the liquid; porosity and the nominal pore size indicates how much space is available for that contact to occur. The thicker a membrane is, the further gases must travel before making contact with the liquid, thus increasing the membrane resistance to the diffusion of gases. A recent study (Vanneste et al., 2017) characterized 17 hydrophobic membranes for membrane distillation (MD). The membrane manufacturer data and results from that study are summarized in Table 2-1, and Figure 2-3 depicts the vapor flux and hydrophobicity of those membranes.

The majority of the membranes studied by Vanneste et al. (2017) have porosities higher than 70%. The nominal pore size is listed, but the actual pores are not consistent and instead may be larger or smaller. These pores are not tube-like holes, but a matrix of tortuous passages through the membrane. The active layer contacts the stream that water is being recovered from, and the support layer is on the

opposite side to provide mechanical strength.

Table 2-1. Characteristics of gas transfer membranes (Vanneste et al., 2017). For this study, CLARCOR QL822, CLARCOR QP952, and 3M 0.45 μm were used.

| Manufacturer | Model Number | Active layer | Support Material | Nominal Pore Size (μm) | Thickness (μm) | Porosity (%) |
|----------------|--------------|-------------------------------|------------------|-------------------------------------|-----------------------------|--------------------|
| 3M | 0.2 micron | PP ¹ | No | 0.59 ² | 110 | 85 |
| 3M | 0.45 micron | PP ¹ | No | 0.79 ² | 110 | 85 |
| 3M | ECTFE | ECTFE ³ | No | 0.43 ² | 46 | 67 |
| Aquastill | 0.3 micron | PE ⁴ | No | 0.3 | 76 | 85 |
| Celgard | 2400 | PP ¹ | No | 0.043 | 25 | 41 |
| Celgard | 2500 | PP ¹ | No | 0.064 | 25 | 55 |
| CLARCOR | QL218 | ePTFE ⁵ | PP ¹ | 0.2 | 254-305 | 70-85 ⁶ |
| CLARCOR | QL822 | ePTFE ⁵ | PP ¹ | 0.45 | 127-203 | 70-85 ⁶ |
| CLARCOR | QP952 | ePTFE ⁵ | PES ⁷ | 0.45 | 150-300 | 70-85 ⁶ |
| CLARCOR | QP955 | ePTFE ⁵ | PES ⁷ | 0.2 | 127-305 | 70-85 ⁶ |
| CLARCOR | QP961 | Oleophobic ePTFE ⁵ | PES ⁷ | 0.1 | 76-203 | 70-85 ⁶ |
| CLARCOR | QM902 | ePTFE ⁵ | No | 0.45 | - | 70-85 ⁶ |
| Osmonics Corp. | PP22 | PP ¹ | No | 0.22 | 150 | 70 |
| Osmonics Corp. | TS22 | PTFE ⁵ | PP ¹ | 0.22 | 175 | 70 |
| Osmonics Corp. | PVDF | PVDF ⁹ | No | 0.4 | 160 | - |
| Pall Corp. | 0.2 micron | PTFE ⁵ | LDA ⁸ | 0.2 | 179-246 | - |
| Pall Corp. | 0.45 micron | PTFE ⁵ | LDA ⁸ | 0.45 | 191-257 | - |

¹ PP: Polypropylene; ² Bubble Point Pore Diameter; ³ ECTFE: Ethylene Chlorotrifluoroethylene; ⁴ PE: Polyethylene ; ⁵ ePTFE: elongated polytetrafluoroethylene; ⁶ Estimate of manufacturer; ⁷ PES: Non-woven polyester; ⁸ Non-woven polypropylene; ⁹ PVDF: Polyvinylidene difluoride.

Vapor flux through the 3M and CLARCOR membranes was the highest for the membranes tested by Vanneste et al. (2017). High flux indicates that these membranes may effectively deliver gases to liquid growth media during our gas transfer study and bacterial growth trials, while their hydrophobicity would prevent pore space wetting. The flat-sheet membranes chosen from Vanneste et al. (2017) for use in this study were CLARCOR QP952, CLARCOR QL822, and 3M PP 0.2 μm .

Membrane contact angles were measured by Vanneste et al. (2017) with membranes attached to a flat surface, and a camera that captured the water droplet being repelled from the membrane surface. This procedure was not conducive for measuring the contact angle of the small hollow fibers because they are not flat, but round. The manufacturers state what materials are used for the fibers, and simply define them as hydrophobic. PP and PTFE are both used as the active layer for several membranes, and both materials produced varying contact angle measurements. Part of the difference may be due to surface characteristics of the different membranes, which plays a significant role in a surface's ability to repel water (Quééré, 2002; Zheng & Lü, 2014). Cases of super-hydrophobicity on plant surfaces often rely on micro-sized structures that create contact angles in excess of 150°, versus chemically enhanced surfaces that yield values nearer to 120° (Barthlott et al., 1997).

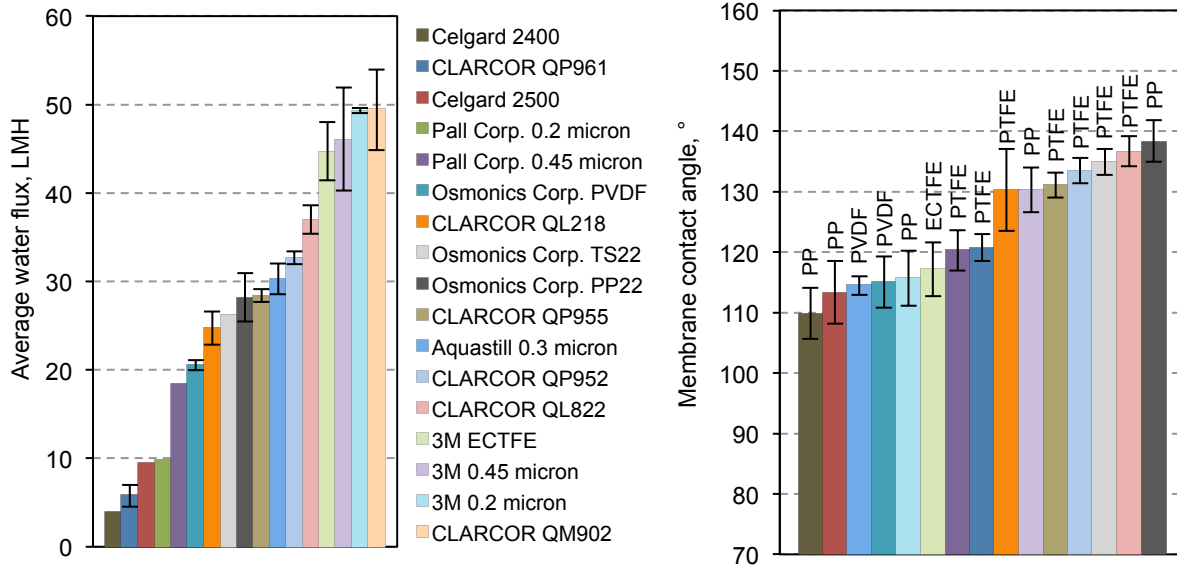


Figure 2-3. Left: Comparison of vapor flux across the 17 membranes used for MD; system operated with the feed stream 40 °C warmer than the distillate stream, 1.6 LPM countercurrent flow rates, and 1 g/L NaCl in the feed solution. Right: Contact angle comparison for the same 17 membranes (Vanneste et al., 2017). Error bars on average water flux and membrane contact angle graphs represent the standard deviation of four measurements and ten measurements, respectively.

CHAPTER 3

MATERIALS AND METHODS

A membrane-based bioreactor was designed and built for experimental growth trials. This chapter discusses design, safety of operation, general design choices, material evaluation with respect to using pure gases, and the methods used to test membranes before their use during growth trials. Preparation of bacterial samples used for inoculation of the reactor, operation of growth trials, and the methods used to monitor the progress of growth trials are also described.

3.1 Membrane-Based Bioreactor Design

Bench-scale design concepts were produced based on previous experience with MD processes, and the following goals:

- The ability to safely manage methane and oxygen within the system,
- Phase separation of gases and liquids using membranes,
- Diffusion of gases into liquid growth media for use by bacteria,
- Media isolation from the atmosphere,
- Control of gas and liquid flows, as well as temperatures in the system,
- Continuous monitoring of dissolved oxygen levels, and
- Consideration for known challenges presented by operations in microgravity.

A study found that to detonate gas mixtures, the critical energy required for mixtures of 40% methane and 60% oxygen was 57 joules, which is two orders of magnitude higher than any other hydrocarbon (Matsui & Lee, 1979). In the presence of atmospheric oxygen concentrations (20% O₂), methane gas is flammable if mixtures fall within the range of 5-15% by volume (Praxair, 2016). Isolation of each gas, instead of mixing, is desirable to prevent dangerous mixtures of gas.

Gas bubbles immersed in water on Earth experience buoyancy, a force opposing gravity that causes gas bubbles to rise due to density differences. Gas bubbles may coalesce within the system to create gas mixtures of unknown content. Isolating gases from liquid growth medium via membranes manages these potential risks by separating gas and liquid phases, and preventing the formation of gas bubbles. Membranes are a vital core component of this reactor's design because they facilitate contact between the gases and the liquid growth medium into which gases dissolve.

3.1.1 System Design

The central tank reactor for this system was a 3.2-liter cylindrical acrylic tank. The lid, sealed with a rubber gasket, incorporated a headspace exhaust port and sealed ports for temperature and optical dissolved oxygen (ODO) probes. Isolation from the atmosphere was important because the mixed bacterial culture is capable of fixing nitrogen (Mango Materials, 2016), which would prohibit PHB

production. Fluid loops delivered dissolved gases from the membrane modules via entrance/exit ports in the reactor tank. A magnetic stir bar and stir plate provided mixing in the tank.

The bacteria grow best at 30 °C (Mango Materials, 2016). Instead of using a direct-contact heat element, a standard infrared heating lamp provided heat to the reactor via radiation with very minimal fluctuations. Half of the reactor chamber was covered with a layer of reflective bubble wrap to insulate the tank and reflect the radiation back through the growth medium to further warm it. To isolate this ignition source, the heat lamp was located inside the fume hood in the opposite corner from where oxygen and methane are supplied to and exhausted from the membrane modules.

Liquid medium circulated within the system in two different loops via gear micro-pumps chosen to avoid generation of excess heat and the potential for cell lysis. To measure liquid flow rate, rotameters precalibrated for water flow were read manually. The liquid pressure upstream of the membrane modules was monitored using a pressure gage to observe hydraulic pressure on the membrane. The loop was constructed with a combination of clear polyethylene tubes and compression fittings made from polypropylene (PP), with the exception of piping directly connected to the pump head, which was made of stainless steel. System configurations utilizing parallel and series module configurations are shown in Figure 3-1 and Figure 3-2. Once these system configurations were assembled, the total liquid volume in the system was ~3.5 liters. An image of the assembled bioreactor during a growth trial with modules connected in parallel can be found in Appendix A.

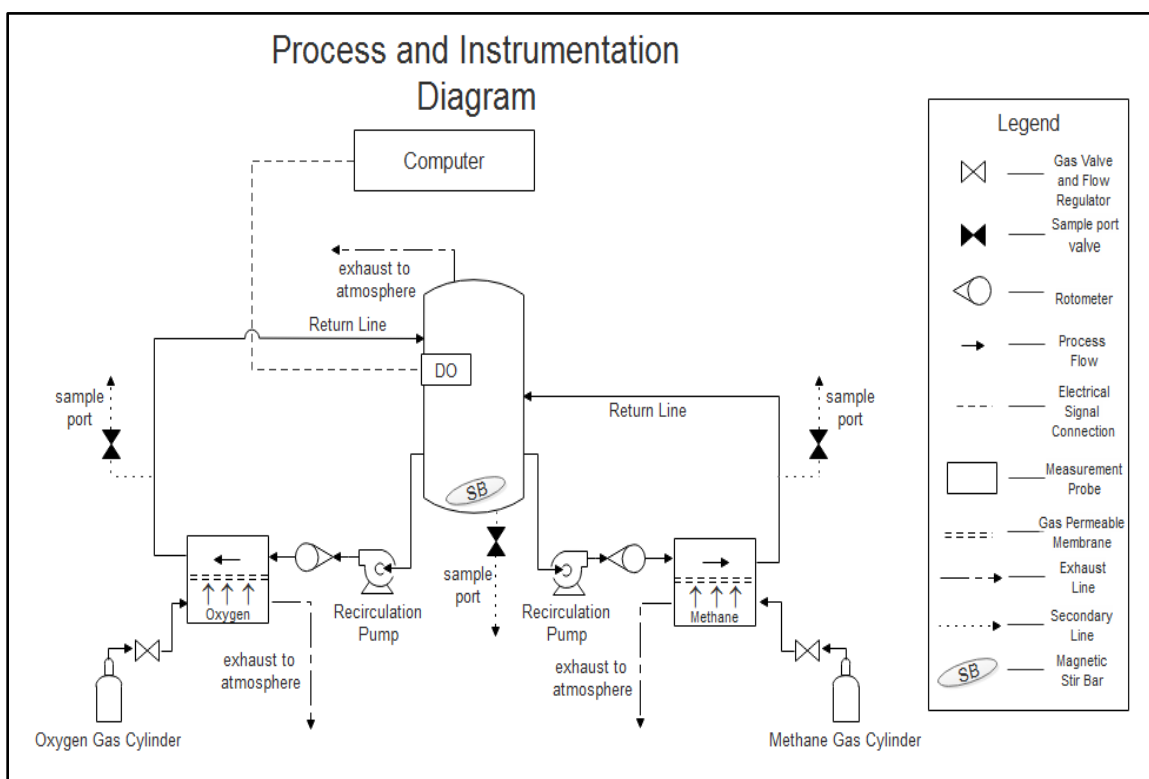


Figure 3-1. Diagram of the bioreactor operated with membrane modules in a parallel configuration. Each module delivers a pure gas, and gas streams do not mix.

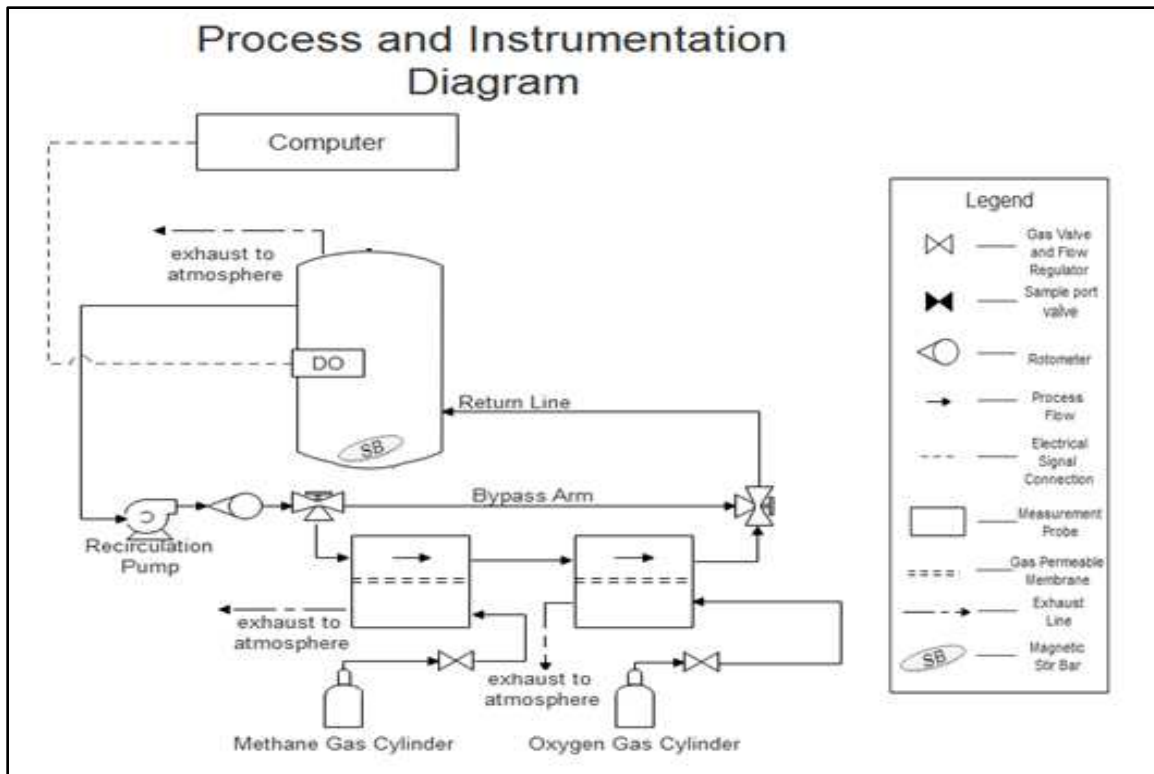


Figure 3-2. Diagram of the bioreactor operated with membrane modules in a series configuration. Either methane or oxygen is delivered and exhausted to the atmosphere in each membrane module to prevent mixing of gases. In this drawing the methane is delivered first, but the operation was also reversed to deliver oxygen first.

3.1.2 Initial Membrane Selection

Flat sheet (FS) membranes that performed well in the study by Vanneste et al. (2017) were used, in addition to hollow fiber (HF) modules from Liqui-Cel, Microdyn, Minntec, and PermSelect. FS membranes were chosen based on the vapor flux performance, hydrophobicity, cost, and robustness of each membrane. FS membranes are replaceable, cost \$5-20 per module, and some have backing layers that increase robustness. In comparison, the hollow fiber modules ranged in cost from \$300 to \$1500, and fibers within the modules are not replaceable.

The FS and HF membranes tested are hydrophobic, and their structures are microporous. The PermSelect HF module uses a dense fiber that is permeable to gas, but its fiber pore space is much tighter than the other HFs. For all membranes, if pressures exceed the liquid entry pressure of water (LEPW), the membrane pore space may flood. Maintaining separation of gas and liquid requires that neither is pressurized enough to pass through the membrane and cause gas and liquid mixing. Manufacturers and membrane characteristics, including water vapor flux performance of the FS membranes at a temperature difference of 40 °C, are summarized in Table 3-1. Selected HF membrane modules from 3M, Minntec, Microdyn, and PermSelect were not previously used for MD and were not characterized for vapor flux, which indicates transport of water vapor across the membrane. Contact angles were also not measured for HF modules, but manufacturers report that their fibers are

hydrophobic.

Table 3-1. Characteristics of flat-sheet membranes used for testing in this study. Data for the FS membrane are from (Vanneste et al., 2017)

| <i>Manufacturer / Membrane</i> | <i>Material / Support Layer</i> | <i>Module Type</i> | <i>Contact angle (°)</i> | <i>Pore size⁴ (μm)</i> | <i>Porosity⁴ (%)</i> | <i>Thickness (μm)</i> | <i>Vapor Flux (LMH)</i> |
|--------------------------------|-------------------------------------|--------------------|--------------------------|-----------------------------------|---------------------------------|-----------------------|-------------------------|
| CLARCOR / QL822 | PTFE ¹ / PP ² | FS | 136.7 | 0.45 | 70-85 | 127-203 | 35.14 |
| CLARCOR / QP952 | PTFE ¹ / Polyester | FS | 133.49 | 0.2 | 70-85 | 150-300 | 32.48 |
| 3M / PP 0.45 μm | PP ² / N/A | FS | 115.68 | 0.79 | 85 | 110 | 46.1 |
| 3M X50 2.5x8.0 | PP ² | Porous HF | n/m | 0.04 | 40 | 80 | n/m |
| Microdyn MD 020 CP 2N | PP ² | Porous HF | n/m | 0.2 | 80 | 400 | n/m |
| Minntec FiberFlo MCV-030 | PP ² | Porous HF | n/m | 0.3 | 40 | 56 | n/m |
| PermSelect PDMSXA 0.1 | PDMS ³ | Dense HF | n/m | N/A | N/A | 55 | n/m |

¹Supported polytetrafluoroethylene; ²Polypropylene; ³ Polydimethylsiloxane; ⁴Manufacturer estimate. N/A indicates not applicable; n/m indicates not measured.

3.1.3 Flat Sheet and Hollow Fiber Membrane Modules

FS membranes are housed within modules that facilitate gas and liquid flow within designated channels. Modules previously designed for MD consist of two semi-cells that join together with the membrane sandwiched in the center. The membrane cell is constructed with rubber gasket material that simultaneously seals and forms the rectangular flow channels. Each channel has a mesh spacer that supports the membrane and maintains mixing of the fluid. This is necessary because FS membranes are not rigid, but deform easily; without the spacers the membrane would collapse into the flow channel, restricting gas or liquid flow and reducing the effective membrane area.

The HF modules are made of a bundle of fibers potted on two sides, and enclosed in a tube. The liquid growth medium can flow either on the shell or lumen side of the fibers via ports in the tube. In this study, we operated the HF modules with the growth medium flowing into the fiber lumen, and the gas flowing into the module shell, making contact with the outside of the fibers. Initial tests were performed where liquid flowed through the lumen or the shell. When flowing through the shell, the maximum hydraulic pressure, as recommended by the manufacturer, was reached at a lower flow rate compared to operating the liquid flow inside the lumen (Appendix B). A HF module and a FS membrane module are pictured in Figure 3-3.

3.1.4 Material Compatibility with Methane and Oxygen

Dissolved gas concentrations in the growth medium do not warrant special material considerations. The materials used include polyethylene (PE), polypropylene (PP), nylon, stainless steel,

and acrylic, all of which are non-reactive in contact with dissolved oxygen and methane. This section focuses on contact with gases because they present the greatest hazards within this system and can chemically alter materials.

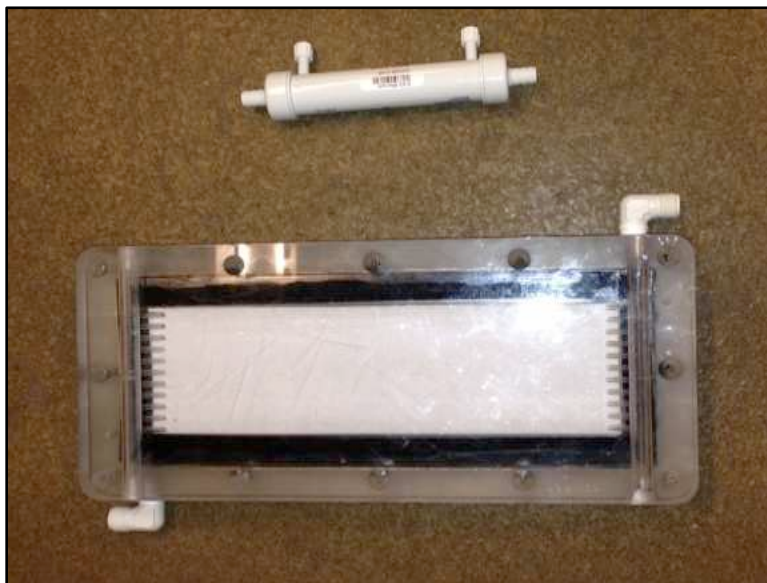


Figure 3-3. Flat-sheet and Minntec hollow fiber module. Flat sheet module dimensions are 16 inches by 6 inches, but surface area of the hollow fiber module is a factor of 10 higher.

Methane is compatible with brass, copper, and PE (Praxair, 2011). Two gas suppliers rate the compatibility of methane with polycarbonate as having insufficient data or not applicable (CellTreat, 2014; Praxair, 2011), and one rated it as acceptable (Holophane, 2011). Polypropylene (PP) is known to be fairly resistant to many chemicals and is listed by Cell Treat© (2014) as being resistant to methane. Based on these material recommendations, the methane gas distribution system included a brass regulator for the gas cylinder, copper line with brass compression fittings, a polycarbonate flow meter, and PE tubing with PP compression fittings used for distribution to polycarbonate modules. Material oxidation and degradation risks were considered acceptable because system operation for the duration of study would be observed.

Oxygen-rich environments may provide enough reactivity to ignite nonmetallic materials that are otherwise considered compatible. The use of materials such as PE is thus dependent on gas pressure, gas temperature, system cleanliness, and the presence of gas ignition sources (Praxair, 2011). PE and PP have compatibility ratings of resistant and unsatisfactory, respectively, as materials for use during direct oxygen contact, with the limitations that conditions not include significant pressure or temperatures exceeding 60 °C (Ineos, 2016; IPEX, 2013). PE tubing was chosen for oxygen delivery, with a combination of PP and brass used for fittings. The modules and gas flow meters are both polycarbonate, a material rated conditionally compatible according to Praxair (2011). Polycarbonate membrane modules designed for use during an MD application were already available, and their use was deemed acceptable.

The membranes themselves were manufactured using polytetrafluoroethylene (PTFE), polyester, PP, and/or ethylene chlorotrifluoro ethylene (ECTFE), depending on the manufacturer. All of these materials are rated A by Chemline Plastics for use with methane or oxygen while temperatures remain below 60 °C (ChemlinePlastics, 2008). Pressurized gases interact differently with materials, but this system was operated at atmospheric pressure, with the exception of one dense HF module that required 10-15 psig.

3.2 Gas Transfer Testing

To characterize the membrane gas transfer, dissolved oxygen (DO) measurements were used to characterize flux and rate of transfer via $K_L a$. Mango Materials determined experimentally that DO concentrations of 5 to 10% saturation, based on pure oxygen gas, are optimal for bacterial growth. DO concentrations are reported in mg/L for this study because Mango Materials and CSM are at sea level and 6000 ft, respectively. Elevation changes atmospheric pressure; thus, the saturation concentrations at Mango Materials and CSM are ~40 mg/L and 33.4 mg/L, respectively, according to average atmospheric pressures of 1.0 atm and 0.803 atm (Toolbox, 2017). Flux and $K_L a$ were determined at oxygen levels in the range of 2-4 mg/L based on the concentrations recommended by Mango Materials.

Funding was not available to purchase a dissolved methane probe; thus, methane gas transfer was assumed based upon oxygen transfer rates. Metcalf & Eddy (2003) confirmed that the ratio of the $K_L a$ of two gases is related to the ratio of diffusion coefficients (D) of the gases according to Equation 3.1 (shown for methane and oxygen), where n is a correction factor (0 to 1) based upon the system being used.

$$\frac{K_L a_{CH_4}}{K_L a_{O_2}} = \left(\frac{D_{CH_4}}{D_{O_2}} \right)^n \quad (3.1)$$

Diffusion coefficients for methane and oxygen in water at 25 °C are 1.88×10^5 and 2.57×10^5 cm^2/s , respectively (Ferrell & Himmelblau, 1967; Witherspoon & Saraf, 1965). If we assume n is equal to one, then the quotient of these values would be 0.731. Experiments by Sheehan & Johnson (1970) observed that gas exchange of oxygen was, on average, 1.37 times higher than for methane; this value agrees with the result of Equation 3.1. In addition to these estimates, methanotrophic growth confirms delivery of methane, because methane concentrations in solution are required for the bacteria to grow.

ODO probes were used to measure DO. The probes used were a Mettler Toledo (Billerica, MA) inPro6850i, and a Vernier (Beaverton, OR) ODO-BTA. Both utilized computerized data logging software provided by the respective manufacturers. A probe was immersed halfway in the reactor filled with deionized (DI) water at all times during testing, and logging software provided real-time data observation in addition to logged data.

3.2.1 Oxygen Gas Transfer Testing Procedure

Two membrane modules were connected to the reactor during the membrane tests: one test

module was used for gas transfer tests and a second module purged oxygen from the DI water in the reactor between tests. A known volume of DI water was used to fill the entire liquid portion of the system. DI water was circulated through the membrane modules by micro-pumps that provided 0.5 to 2.5 LPM, or a friction head pump that provided 1.9 to 9.5 LPM. Maximum flow rate for a specific membrane module depended on what liquid flow produced that membrane's LEPW. Oxygen was removed from the water by sealing the reactor and providing nitrogen gas to the stripping module to purge oxygen from solution. Once the concentration of DO was reduced to <0.5 mg/L, the system was ready for the gas transfer test. Water was maintained at 30 ± 1 °C at all times during testing. Data recording began prior to oxygen gas flow being introduced to the membrane module, and ended after DO concentrations were higher than 20 mg/L. Between tests, the gas transfer module was disconnected from the oxygen source and was dried using compressed air to prevent condensation from impacting transfer results; the other module stripped gas from the reactor at this time.

Testing was always performed using countercurrent flow of gas and liquid streams, with a constant flow of oxygen gas. This procedure was repeated under different liquid and gas flow rates to assess each membrane's performance, and data for each membrane were compiled and analyzed in Microsoft Excel.

3.2.2 Oxygen Gas Stripping Testing Procedure

After gas transfer testing was complete and DO saturation reached 20 mg/L, DO stripping by methane was tested. Methane gas flowed through the module at a rate of 0.5 LPM, and liquid flow was adjusted to 2.0 LPM. Data were collected using the oxygen probe to determine how quickly oxygen was purged from solution when the DO concentration was between 2–4 mg/L.

3.2.3 Determination of K_La and Membrane Flux

Both K_La and gas flux were calculated based on the change in DO measured over time during testing. Equations 3.2 and 3.3 were used to determine gas transfer parameters:

$$K_La = \frac{-d[\ln(\frac{C_{sat}-C}{C_{sat}-C_o})]}{dt} \quad (3.2)$$

$$flux = \left[\frac{dC}{dt} / Area \right] [Volume] \quad (3.3)$$

where C_{sat} represents the concentration of oxygen at saturation, C is the bulk concentration in the DI water at a given time, C_o is the initial oxygen concentrations, area refers to the area of membrane used for gas transfer, and the volume is how much DI water was used in the gas transfer test.

Flux and K_La are both impacted by the flow rates of gas and liquid passing through the module, which impact the concentration difference between liquid in contact with the membrane and the bulk

liquid. If the concentration in the bulk liquid is further from equilibrium, the gas more readily diffuses into the liquid. This was confirmed by data analysis, and can be seen in a graph of gas transfer testing with a FS and HF shown in Figure 3-4. Both graphs are concave to the x-axis, and each has the steepest slope within the first few minutes. This indicates the rate of transfer was greatest in the early phase of the test while the DO concentration in the bulk liquid was lowest, and the rate decreased as the trial progressed and DO concentrations increased. The HF plot is more concave than the FS plot, which may be due to their differences in flux. The data used from these tests to determine flux and $K_L a$ were in the range of 2–4 mg/L DO.

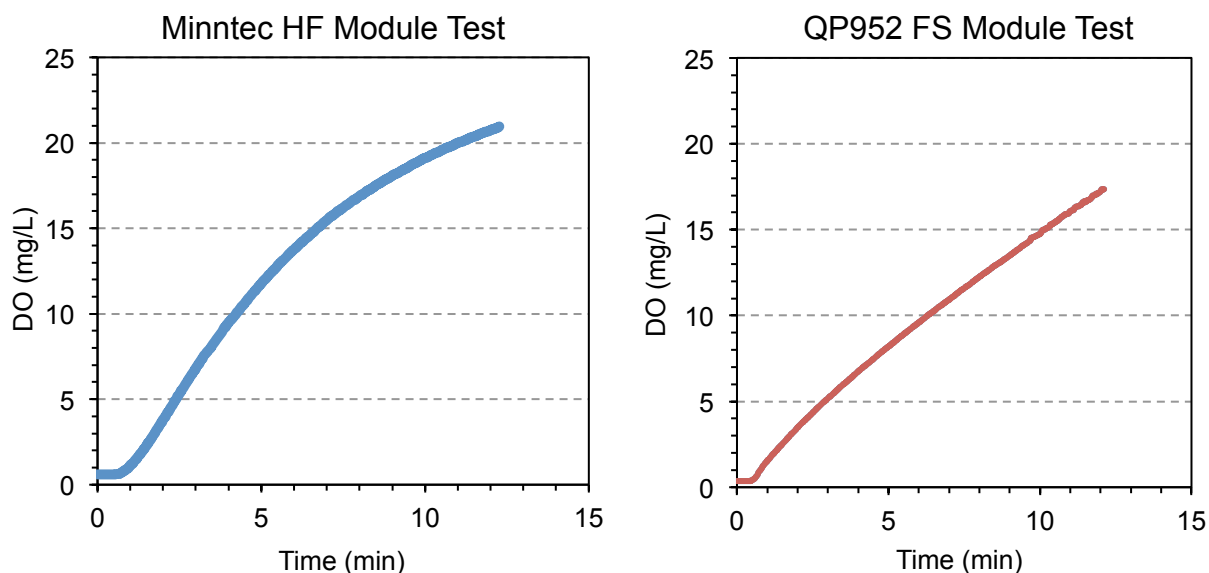


Figure 3-4. Gas transfer test results for a HF and FS module.

3.3 Growth Medium

The solution used for this study is based on a previously published growth medium that successfully facilitated growth of methanotrophic bacteria. The growth medium contained 0.8 mM $MgSO_4 \cdot 7H_2O$, 0.14 mM $CaCl_2$, 1.2 mM $NaHCO_3$, 3.0 mM NH_4NO_3 , 2.35 mM KH_2PO_4 , 3.4 mM K_2HPO_4 , 2.07 μM $Na_2MoO_4 \cdot 2H_2O$, 1.0 μM $CuSO_4 \cdot 5H_2O$, 10 μM Fe-EDTA, and 1 ml trace metal solution [containing, per liter, 500 mg $FeSO_4 \cdot 7H_2O$, 400 mg $ZnSO_4 \cdot 7H_2O$, 20 mg $MnCl_2 \cdot 7H_2O$, 50 mg $CoCl_2 \cdot 6H_2O$, 10 mg $NiCl_2 \cdot 6H_2O$, 15 mg H_3BO_3 , 250 mg EDTA] (Pieja, 2011). The medium was autoclaved and cooled before use in microcosms and growth trials.

3.4 Methanotrophic Culture Microcosms

Mango Materials provided a mixed culture dominated by Type II methanotrophs, including members of *Methylocystis*. This culture was originally sent as a small pellet, and after re-suspension in growth medium, was used to inoculate several microcosms. These microcosms served to inoculate other microcosms.

125 mL bottles with rubber stoppers and metal caps were autoclaved at 135 °C for 20 minutes before use. Aseptic handling techniques were used to transfer 50 mL of growth medium into each bottle. Once in the bottle, the medium was inoculated with 1 mL of suspended methanotrophic growth, and bottles were sealed. Headspace in bottles was then vacuumed out and replaced with a mixture of 40 mL of methane and 40 mL of oxygen. Microcosms were placed inside an incubator set to 30 °C for two days on an orbital shaker table, and then stored in a refrigerator until needed. Microcosms were returned to the incubator and shaker table for an additional two days prior to inoculation of a growth trial to allow for more substantial growth before their use.

3.5 Growth Trial Operation

Prior to operation, without any membrane modules connected, the reactor and its loops were disinfected for an hour using a dilution of 8.25% sodium hypochlorite bleach (1:100), and then washed three separate times by circulating three liters of DI water to remove any remaining bleach. The top was left open for chlorine to escape. Once bleach was washed out, modules were reconnected to the system.

New trials began with modules connected in the system, gases and liquids flowing through the modules, reactor mixing, and 3.25 liters of medium heated to 30 °C using the heat lamp. Temperatures were maintained during all growth trials by moving the reactor closer to or further from the heat lamp. Air pulled in by the fume hood served as a cooling source for the reactor, and was adjusted by altering the height of the fume hood's sliding glass protection door. Methane and oxygen were delivered to the modules, and the system was allowed to reach steady state. Once conditions were stable, the reactor was inoculated with microcosms. Five microcosms were used for inoculation, totaling 250 mL of growth culture. The space remaining in the reactor was then filled with growth solution, and the initial volume was recorded. Initial measurements of liquid flow rate, gas flow rate, reactor temperature, DO, nitrate concentration, and ammonium concentration were recorded. Over the duration of a trial, the system was continually checked to ensure the temperature, DO, gas flows, and liquid flows all remained within their desired ranges.

3.5.1 Pure Gas and Gas Mixture Operation

During operation, pure gases were fed into separate modules and were measured/controlled using manual flowmeters that were factory calibrated for airflow. The actual flows for methane were approximately 75% of the flowmeter reading; oxygen flow did not require correction. While using gas mixtures, gas flows from the flowmeters were combined using a T-fitting and delivered to both modules using a second T-fitting. Actual flow rates were initially set to create gas mixtures of 2:1 (methane:oxygen). As the trial progressed, that mixture was changed by increasing the flow of oxygen. This occurred in the event that the DO was less than 2 mg/L, and the mixture was only allowed to reach 1:1 for safety precautions. The maximum flow used for methane was 0.225 LPM (after correction), and maximum oxygen flow was 0.225 LPM. Exhaust flows were vented to the rear of the fume hood to

prevent contact with any potential ignition source.

3.5.2 *Liquid Flow Rate Alterations*

Each series growth trial used liquid flow rates of 2 LPM, which was maintained throughout the trial. This required only one pump, which was adjusted by hand according to the readings on the rotameter connected in line after the pump. When the reactor was operated in parallel configuration, two pumps were adjusted. The parallel growth trial using pure gases started with a liquid flow in the methane module loop of 2 LPM, which was increased later to 2.5 LPM. The liquid flow rate for the oxygen module loop was first set to 0.5 LPM and steadily increased as the culture depleted more oxygen.

When mixed gases were used, the liquid flow rate was set to 2 LPM for the duration of the trial. When HF modules were used, increase in DO concentration was observed during the growth trial when the flow rates were decreased. This phenomenon was not investigated further during this study.

3.5.3 *Module Draining*

Condensation that occurred in membrane modules due to water vapor crossing the membrane needed to be drained periodically. FS modules were drained via the exhaust ports while the module was tilted until condensate was no longer present in the gas channel; gas exhaust was reconnected afterwards. When hollow fiber modules were connected to the system, they were fixed to the interior of the fume hood. Modules were inclined to allow any condensation in the module to drain from the shell. Gases entered the elevated end of the module and exited in the same tube as the condensate. Gases and liquids were separated by a Y-junction in the exit tubing to ensure gases exhausted via a tube directed to the top of the fume hood away from ignition sources.

3.6 **Measurement Methods**

Samples were taken directly from the top of the reactor throughout the growth trials using a sterile syringe. Samples used solely for optical density (OD) measurements were returned to the reactor to prevent long-term drawdown of the volume. Destructive measurements and water vapor flux across the membrane depleted the reactor's volume as the trial progressed.

3.6.1 *Microbial Growth Measurements*

To capture the microbial growth during a trial, OD was measured at least three times a day. When measuring OD, 20 mL of medium was removed from the reactor and placed into a square glass Hach vial. A HACH DR5000 spectrophotometer measured light absorbance at 595 nanometers (nm). The same jar was filled with 20 mL of milli-Q water; this measurement was used as a blank. An absorbance range of 0.1 to 3.0 is considered accurate for the DR5000, and it saturates at 3.5 abs (HACH, 2005). Dilutions were not used because the readings never saturated. After the sample was returned to the reactor, the vial was washed with DI water, cleaned with a paper towel, and left to dry until later

measurements.

3.6.2 Ammonium and Nitrate Consumption

Ammonium and nitrate served as the nitrogen sources for methanotrophs in this study. Concentrations were measured 12 hours after inoculation, and twice each day until depleted. Samples from the reactor were filtered using 0.45 μm nylon syringe cartridges from MicroLiter Analytical Supplies, Inc. (Suwanee, GA), and then analyzed according to HACH procedures (HACH, 2005). Ammonium was measured using high range and low range TNT 830 and 832 tests, and nitrate was measured using high range and low range TNT 835 and 836 tests. Results were reported by the DR5000 as mg of N per liter for both NH_3 and NO_3^- .

3.6.3 PHB Confirmation Testing

After depletion of both nitrate and ammonium, the methanotrophic bacteria start to produce PHB. Mango Materials accurately measures cellular PHB mass using Fourier transform infrared (FTIR) spectroscopy, but during these trials we used a surrogate measurement that Mango Materials recommended, a bleach digestion. This method compares a sample diluted with water with a sample digested with bleach. Samples were again removed from the system by syringe. An example of this measurement using a 1:1 bleach ratio used 10 mL of sample, either diluted with 10 mL of milli-Q water or mixed with 10 mL of household bleach (8.25% sodium hypochlorite). The bleach dilution mix was allowed to digest for 20 minutes, and OD measurements were taken for both samples. The bleach ratio is a comparison of the OD as shown in Equation 3.3:

$$\text{Bleach Ratio} = \frac{\text{OD of Bleach digestions}}{\text{OD of diluted sample}} \quad (3.3)$$

When optical density increased beyond 2.5 and 3.0 abs, dilution was increased to 1:3 and 1:9, respectively. Increased dilutions were needed when cells did not digest fully. This is not an exact measurement of PHB content, only a surrogate that indicates the likelihood of PHB in the cells. Above a ratio of 0.1, the sample was considered “likely” to have PHB; as the ratio value increases, the likelihood of PHB is increased (Mango Materials, 2016). Once the bleach ratio stabilized, 250 mL samples were taken, centrifuged at 4000 rpm in 50 mL Falcon tubes, and pellets were combined into one 50 mL tube. The combined pellets were shipped overnight in a package containing a half-gallon plastic bag with several ice packs and bubble wrap to protect and insulate the samples.

Mango Materials analyzed these samples first with FTIR using a Nicolette iS10 from Thermo Scientific (Lafayette, CO) to analyze samples. Blank readings were taken prior to all sample readings to correct for equipment background reading, and samples that contained 100% and 60% PHB from previous growth trials were used to calibrate the model (Mango Materials, 2016). The results were analyzed for PHB using the method described by a study of a partial least squares regression (Mevik &

Wehrens, 2007). Gas chromatography was used by Mango Materials to calibrate the FTIR results prior to these measurements.

3.7 Sources of Error

All measurements have some level of variability, either caused by the measurement devices themselves, variability in the operation of the system, or uncontrollable changes. This section discusses errors, and how to address them during future operations.

3.7.1 Manual Control Methods

All systems within this bench-scale system were manually controlled, with the exception of the temperature and ODO probes monitoring the system. The flow meters for oxygen and methane in particular visibly fluctuated over time on the order of 0.01–0.02 LPM, and often needed to be corrected. Delivery of these gases to the system is paramount, and when flow of either gas decreased or increased, concentration differences changed; in the experiments with mixed gases these fluctuations altered the partial pressures of each gas in the membrane modules. Mitigation of this error would involve the use of a gas flow controller instead of valves. Having a reliable way to measure gas composition would aid in creating more accurate gas mixtures as well.

Pumps were manually controlled and the flow rate was adjusted based on readings from a rotameter with a resolution of 0.25 LPM. Computer control and monitoring by use of a digital flowmeter and a more precise rotameter would allow the system to be altered remotely, and with increased precision.

3.7.2 Methane Measurements

Inline dissolved methane sensors were cost-prohibitive for this phase of the project. No data were collected for the dissolved methane concentrations, but dissolved methane was assumed based on the culture growing and producing PHB. Limited dissolved methane would slow the bacterial growth.

During flux testing, liquid samples were sealed in vials to allow methane to partition into the headspace, but subsequent gas chromatography of headspace samples did not yield consistent, measureable methane concentrations. System operations would benefit from a methane probe to monitor dissolved methane concentrations.

3.7.3 Bacterial Growth Measurements

OD measurements varied as the cells settled in the measurement vial. The OD readings increased on the order of 0.005 to 0.02 absorbance units while cells were still moving from mixing due to the transfer of liquid into the HACH vial. If the culture was left in the vial for more than 10 minutes before a measurement, cells began to settle to the bottom and decreased by the same range as the culture settled over ten minutes. Data reported the greatest reading from each culture sample to ensure

consistency. Having an in-system turbidimeter would remove the need to eliminate samples from the reactor and would allow for continuous observation of the growth.

3.7.4 *PHB Confirmation Testing*

Bleach digestion tests required 20 mL of culture from the reactor. Gradual drawdown of the reactor volume resulted in headspace that may have influenced the growth of bacteria. The bleach itself varied based on how old the bleach was, when it was first opened, and the quality of the bleach, which resulted in varying degrees of hypochlorite digestion over the 20-minute reaction time. The digestion could not be run longer because this may result in digestion of the PHB itself, introducing additional error and variability.

Bacteria were still active when they were removed from the reactor. Samples were centrifuged in 50 mL Falcon tubes, supernatant was removed, and the bacteria pellet that remained was sent same day on ice overnight to Mango Materials for PHB analysis the following day. Methanotrophic bacteria are able to fix nitrogen from the atmosphere, and will consume PHB in their cells when methane is not present (Rostkowski et al., 2013). The potential impacts of time between harvesting, processing, shipping, and measurement of PHB mass in bacterial cells were not investigated. Using the FTIR method for PHB analysis at CSM would eliminate any error that cell processing and shipping introduces.

CHAPTER 4
RESULTS AND DISCUSSION

Membranes were used in this bioreactor design to provide bacteria with oxygen and methane for growth. Gas transfer capabilities of membranes were investigated using different membrane models and types, and various operational conditions. Membrane gas transfer performance was compared using the rate of gas transfer measured as $K_L a$, and flux while the dissolved oxygen (DO) concentration was between 2–4 mg/L. Results of growth trials provide confirmation of whether membranes provide enough dissolved gases so that bacteria will grow and produce PHB.

4.1 Membrane Gas Transfer Results

To compare performance, each flat-sheet (FS) and hollow fiber (HF) membrane was tested for gas transfer. Flux normalizes gas transfer by the area of the membrane. Oxygen flux results for each membrane are summarized in Figure 4-1.

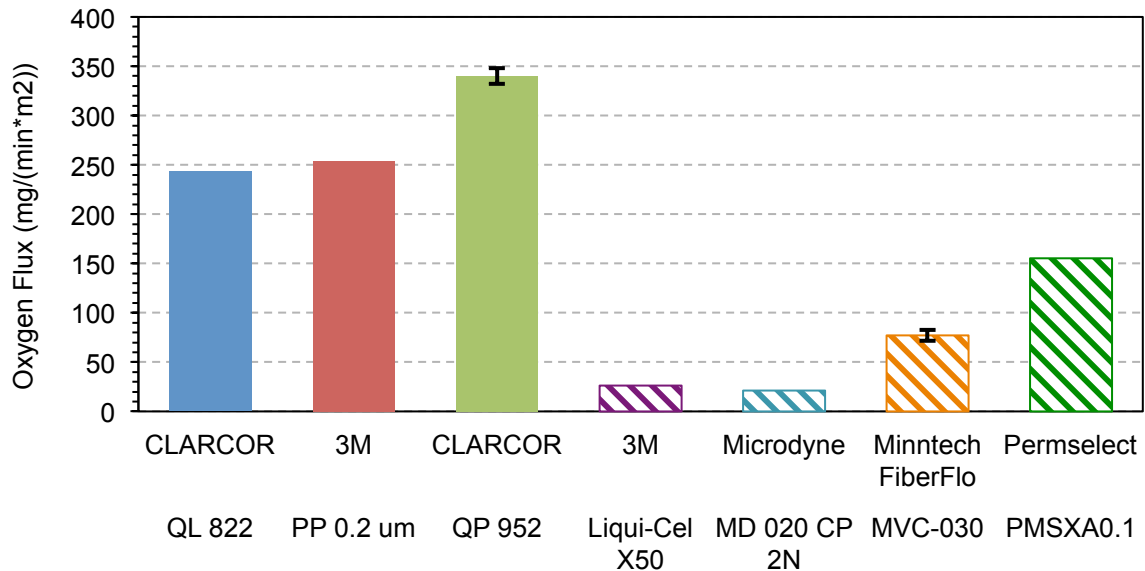


Figure 4-1. Comparison of membrane gas flux; FS represented as solid bars, and HF as hatched bars. Oxygen flux was calculated in the concentration range from 2 to 4 mg/L DO. Tests were performed with liquid flow rate of 2.0 LPM, and gas flow rates of 0.5 LPM. Error bars represent standard deviation based on three tests under the same conditions.

Oxygen flux results indicate that FS are more effective for gas transfer per square meter than HF, with QP952 having the highest flux of 340 mg/(min*m²). This result was counterintuitive considering that the FS membranes are thicker than the HF membranes, with the exception of the Microdyn HF, which was the thickest of all the membranes. However, the porosities of the FS membranes were approximately double those of the HF membranes (again, excepting the Microdyn HF), which may partially account for

the larger flux values. Membrane operation does not allow gas bubbles into the liquid medium, thus, mass transport occurred via diffusion and not volumetric flow through the membrane. The lowest flux values were from the Liqui-Cel and Microdyn modules, and each has an obvious disadvantage with respect to diffusion. The Liqui-Cel module has the smallest pore size of 0.04 μm , and the reduced space within each pore may have caused slower diffusion rates within the membrane. With a membrane thickness of 400 μm , the Microdyn module has the longest passages through the membrane, thus increasing the time required for oxygen gas to diffuse through the membrane. If we compare the Minntec and Liqui-Cel modules, they are very similar with respect to their material and porosity (PP and 40%). However, the Liqui-Cel module has tighter pores (0.04 vs. 0.3 μm) and was an additional 24 μm thicker (80 vs. 56 μm). These two changes in membrane characteristics are the primary differences, and results show that the Minntec module with a thinner membrane and larger pore spaces has three times the flux of the Liqui-Cel module.

Of the HF modules, the PermSelect had the highest flux. The oxygen in the PermSelect module was under pressure (15 psig), and Henry's Law defines the equilibrium (saturation) concentration of a gas in solution using the partial pressure of the gas. If the pressure of the gas increases from 1-2 atm of pressure, then the saturation concentration of that gas in solution doubles. While gas was under pressure in the PermSelect module, C_{sat} increases according to the pressure being used, and Equations 2.3 – 2.5 all show that the difference between C_{sat} and C_w increases. This causes an increase in oxygen flux and explains the PermSelect's increase in gas transfer while under pressure.

Although the FS have higher oxygen flux than the HF, FS modules available for this study provide surface areas one or two orders of magnitude smaller than the HF modules. Increasing the membrane surface area increases gas transfer overall, as indicated by the calculated K_La values, which are based on the same data as flux but reflect the module's rate of gas transfer. Higher K_La values mean the water used for testing became saturated more quickly. Results of K_La tests are summarized in Figure 4-2.

Compared to FS, higher K_La values are expected with HF based solely on their higher surface areas, which range from 0.1 m^2 to 1.4 m^2 . The QP952 membrane module has an area of 0.0193 m^2 , an order of magnitude smaller than the smallest HF module, but its K_La is nearly two-thirds that of the Microdyn module (0.1 m^2). This indicates that the flux of the FS membrane compensates for this specific module's reduced surface area. Increasing membrane area of the FS membrane by using a spiral wound module would likely increase the K_La value beyond that of the Liqui-Cel module.

The Minntec and PermSelect modules have similar K_La , but are different kinds of HF. PermSelect is a dense hollow fiber type with a surface area of 0.1 m^2 , and can operate under gas pressure; the K_La value in Figure 4-2 resulted from applying 15 psig of pressure for oxygen, allowing oxygen to permeate through the HF, but did not pass bubbles into the deionized water. The Minntec HF is a porous membrane that cannot operate under pressure because gas bubbled through the membrane at one or two psig. It has a surface area twice that of the PermSelect, but their K_La values are very similar.

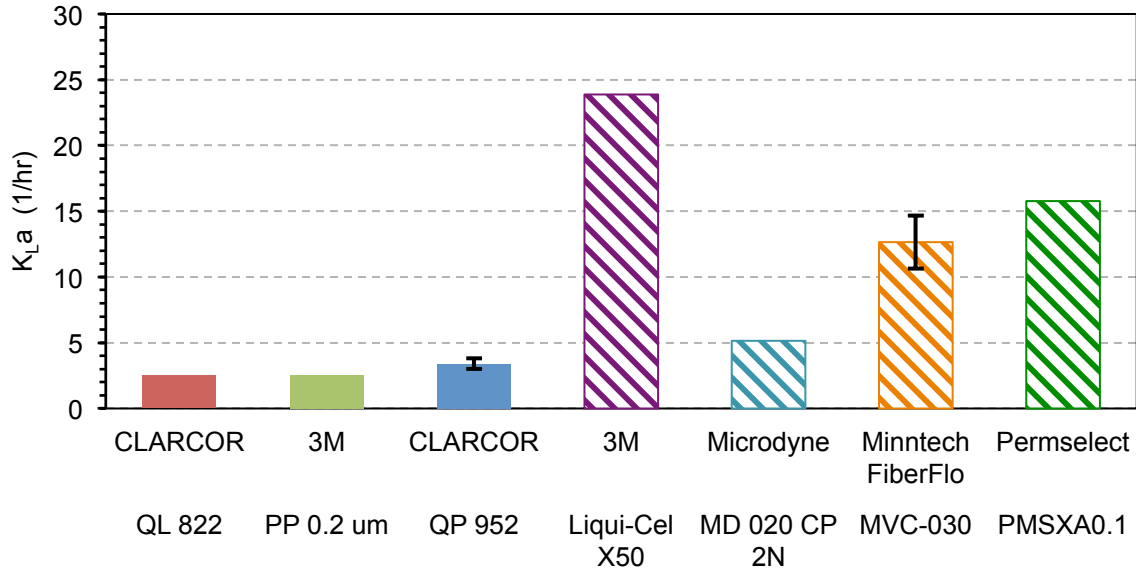


Figure 4-2. K_{La} values calculated for membranes: FS are solid bars, and HF are hatched bars. Testing was performed with liquid flow rate of 2.0 LPM, and gas flow rates of 0.5 LPM. The K_{La} value was obtained from data within 2-4 mg/L. Error bars represent standard deviations based on three tests under the same conditions.

The membrane area contained within the volume of a specific module, reported as m^2/m^3 , is known as “packing density”. Using modules with higher packing density reduces the space those modules require to provide enough membrane area for sufficient gas exchange. The packing densities of modules are presented in Figure 4-3. For comparison, the FS module for this study had a packing density of $6 m^2/m^3$; it is not included in the figure because it is not representative of the FS modules that would be used if this system were upgraded to pilot or full scale. However, the packing density of a commercially available spiral-wound membrane (Evonik MET) is provided for comparison in Figure 4-3.

4.1.1 Operational Changes

Gas transfer is driven by the difference between the bulk liquid concentration and the saturation concentration. This difference remains high if the bulk liquid in the module has a short residence time and does not saturate with gas while in the module. Based on this concept, we speculated that changing the liquid flow rate would impact gas exchange in the system. Figure 4-4 depicts the results of gas exchange tested under liquid flow rates of 0.5 to 2.5 LPM, and 0.5 LPM oxygen gas flow with the CLARCOR QP952.

Results of liquid flow variation tests confirm that gas exchange (both flux and K_{La}) of the FS membrane increased when the liquid flow increased. Increasing the liquid flow by a factor of five increased the oxygen flux by a factor of three, and K_{La} increased by a factor of two. The gas flow rate was varied during testing as well, but results were not consistent with the expected flux and K_{La} values for this membrane, likely caused by membrane wetting; results from these trials are provided in Appendix C. Future testing should include the use of inline gas measurement devices to determine whether gases are

being substantially depleted as they flow through the membrane modules as this will impact gas transfer in the system.

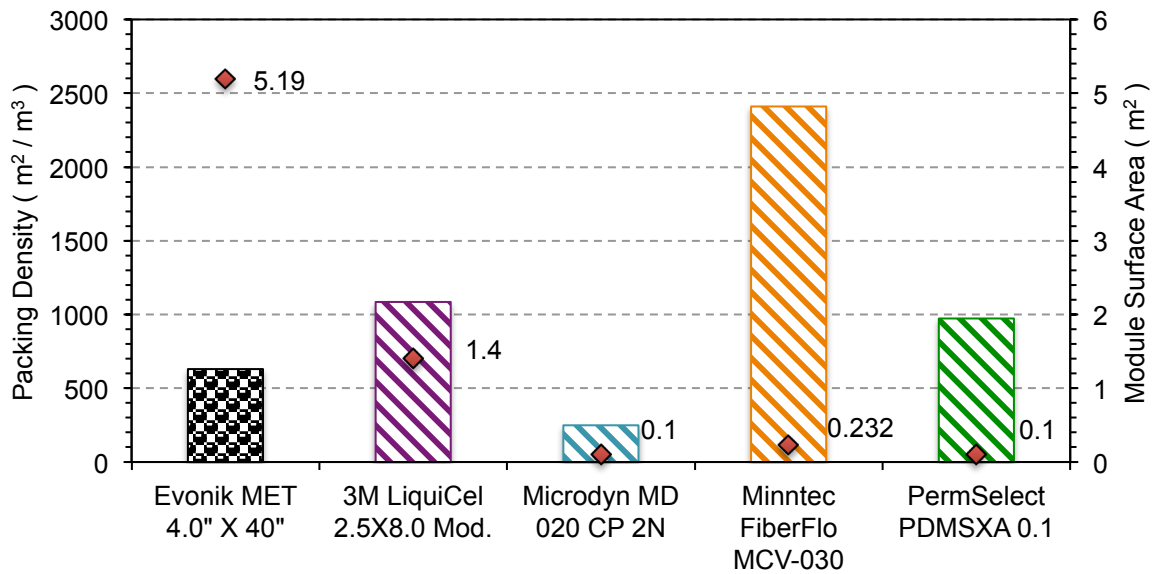


Figure 4-3. Comparison of packing density for the HF modules used in this study (hatched bars) and a FS spiral wound module (dotted bar). Columns indicate the packing density, and the red diamond points indicate the total surface area of each module.

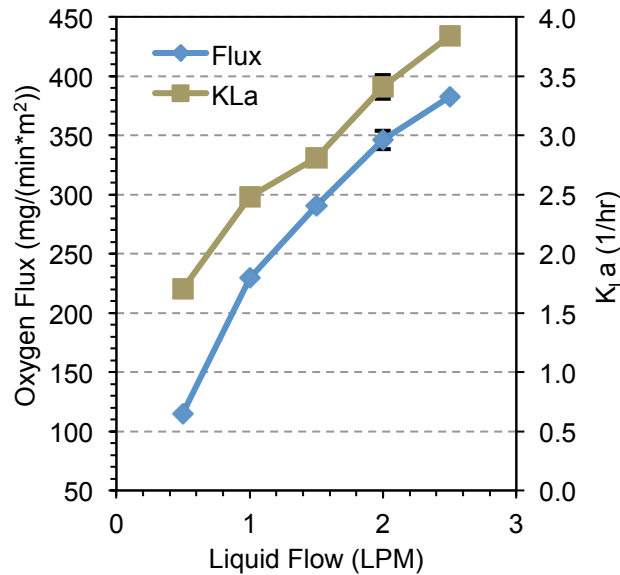


Figure 4-4. Gas exchange of CLARCOR QP952 at different liquid flow rates; gas flow rate was set to 0.5 LPM for all tests. Standard deviation is represented by error bars, and was calculated from three tests.

The flux through the FS membrane was much higher than the HF modules at the same flow rates, but HF modules could be used with much higher flow rates. Results of HF oxygen flux using variable liquid flow rates and oxygen gas flow of 0.5 LPM are compared in Figure 4-5.

The flux in general increases with increasing liquid flow. The exceptions are the highest liquid flow rates used in the Liqui-Cel module, and PermSelect module; these final data points suggest flux decreased. The membrane may have become wet at the highest flow rate, as discussed in section 4.1.2. Of the porous HF modules at atmospheric pressure, Minntec had the highest flux of 111.5 mg/(min*m²).

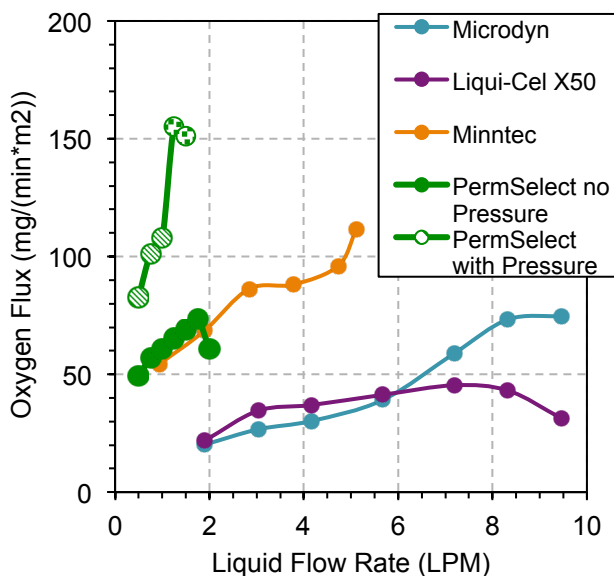


Figure 4-5. Flux comparison of HF membrane at various liquid flow rates; gas flow rate was set to 0.5 LPM. Filled data points represent conditions with gas at atmospheric pressure during operation. Hatched points and dotted points were obtained while pressurizing the oxygen gas at 10 psig and 15 psig, respectively, in the module during testing by restricting flow at the outlet of the HF module.

PermSelect is a dense fiber type with testing conditions that included oxygen pressurized from 5-15 psig in the shell of the module. With applied gas pressure, PermSelect's flux was the same order of magnitude as the flux of the FS, while the fluxes for porous HF were an order of magnitude lower than for the FS type membrane, despite increasing the flow rate through these modules substantially. Flux in the pressurized PermSelect module, 151.2 mg/(min*m²), was the highest of the HFs. Dense HFs require pressure to function optimally because they do not have large pore spaces like porous fibers, but are still permeable to gases. The pressures applied to this module during each test were slightly less than that required for bubbles to penetrate the membrane, which were tested experimentally.

Calculations of K_La for the HF modules (Figure 4-6) revealed the same trend as flux. Higher K_La values compared to the FS membranes were the result of larger surface areas in the HF modules. The Liqui-Cel module, with a surface area of 1.4 m², had the highest K_La of all the HFs with a maximum of 38.8 hr⁻¹. This is comparable to the K_La values of 40 hr⁻¹ reported by Mango Materials for a four-liter bench-scale gas sparging reactor that uses paddle mixing (Mango Materials, 2016).

Increasing liquid flow rates by a factor of four increases K_La by a factor of two on average for the porous HF modules. The PermSelect module results indicate a rate increase when the oxygen pressure

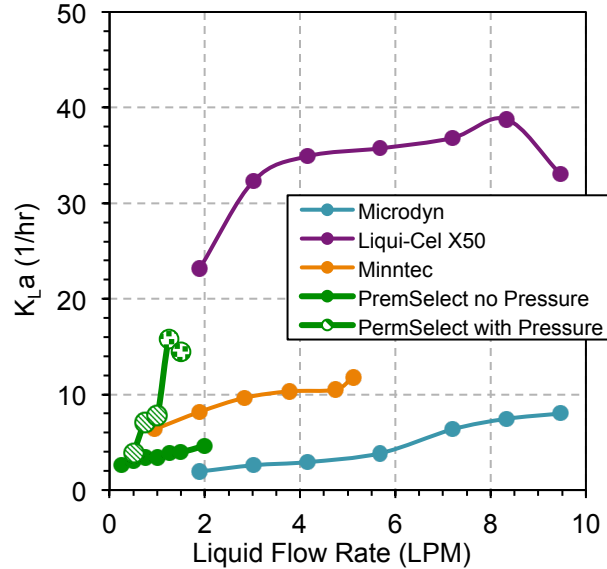


Figure 4-6. K_La calculated for HF membranes at different liquid flow rates and 0.5 LPM of oxygen. Filled data points represent conditions with gas at atmospheric pressure during operation. Hatched points and dotted points were obtained while pressurizing the oxygen gas at 10 psig and 15 psig, respectively, in the module during testing by restricting flow at the outlet of the HF module.

was increased from 10 to 15 psig. All liquid flow increases were accompanied by increases in liquid pressure (Figure 4-7). The decreased gas exchange in the Liqui-Cel module at the highest flow rate may be due to the increase in pressure causing membrane wetting. The Minntec and Microdyn modules did not exhibit the same decrease in gas exchange when fibers were under pressure, possibly due to different fiber characteristics such as higher hydrophobicity that protects the pore spaces from wetting. However, the HF hydrophobicity is unknown because contact angles were not provided by the manufacturer and were not measured at CSM. The Liqui-Cel module also contains more surface area (1.4 m^2 vs. 0.2323 m^2), which may have allowed more water vapor through the membrane, which may have condensed in the shell and wet the fibers, thus decreasing gas transfer.

4.1.2 Hydraulic Pressure on the Membrane, Wetting, and Fouling

Liquid pressure can cause liquid entry into the pore space, resulting in the membrane wetting and increasing the membrane's resistance to gas transfer. Previous studies focused on MD applications that rely on vapor flux indicate that when pressure increased to the point of liquid entry pressure of water (LEPW), the vapor transport through the membrane stopped (Cath et al., 2004). Pressure on the lumen causing membrane wetting would explain the decrease in gas transfer because pores with water inside them do not readily allow gas exchange. It is likely that water vapor from the liquid crossed the membrane and condensed on the spacer in the gas channel, progressively causing wetting over the course of testing.

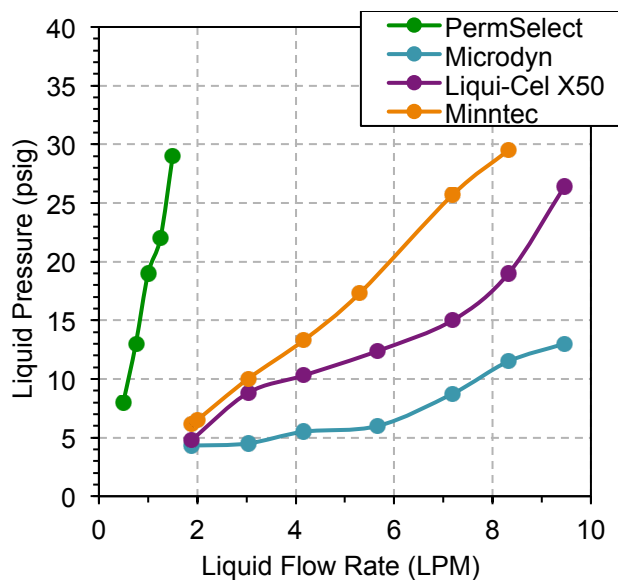


Figure 4-7. Liquid pressures generated by increased flow rates in HF modules. Manufacturer-recommended operational pressure is below 30 psig except for PermSelect, for which less than 45 psig is recommended.

Wetting impairs gas transfer of the membrane by covering pore spaces with water, creating a boundary that prevents gas from entering the pore space of the membrane. Biological fouling on the liquid side of the membrane can also cover pore space, which has the same effect on gas transfer. Gas transfer testing was performed on the CLARCOR QP952 membrane while it was brand new, after water vapor had condensed on it, after wetting was dried, and after two different growth trials fouled the membrane. The results from these tests are depicted in Figure 4-8. Wetting of the membrane resulted in a substantial reduction in gas transfer, as did the wetting and fouling that occurred during a pure gas series growth trial. The mixed gas membrane fouling was not as substantial, and did not appear to be as wet upon inspection. Membrane flux was recovered from the wetted membrane after drying. These results indicate the importance of maintaining a dry, unfouled membrane surface.

4.1.3 Growth Trial with Pure Gases and Flat Sheet Modules in Series

Growth trials with modules in series revealed additional considerations for operation of this system. Trials performed with methane in the first module and oxygen in the second, or in reverse order, were not successful in growing methanotrophs that depleted all of the ammonium or nitrate. Without nitrogen limitation, these bacteria do not produce PHB. Thus, these trials were not considered successful, and changes to the system were required.

DO was not measured during this trial because a reliable oxygen probe was not available for testing. Growth trials were performed without the benefit of this information, and only temperature and OD were observed. This information confirmed that some methane entered the system because bacteria grew, and the OD of these growth trials is depicted in Figure 4-9 as a function of time. OD measurements

for trials two and three are not consistent with the method used for the remainder of the study, but used a 200- μ L quartz cuvette; this vial was broken and the method was changed.

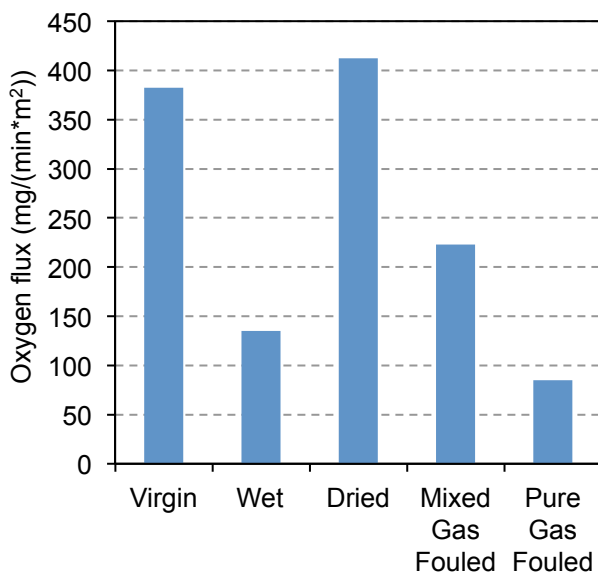


Figure 4-8. Oxygen flux results from CLARCOR QP952 testing under different membrane states. Oxygen flow rate was 0.5 LPM, and liquid flow rate was 2.5 LPM. Fouled membranes were used in growth trials operating with mixed or pure gases prior to gas exchange testing; pure gas operation fouled the methane module.

In all three trials, ammonium and nitrate were never fully consumed, and PHB was never produced. We concluded that methane was purged from solution, causing low dissolved methane concentrations that did not support sufficient growth and PHB production. Henry's Law states that the solution will reach equilibrium with the gas at the gas/liquid interface, thus, if pure gases are used, DO will purge from liquid to gas in the methane module to achieve equilibrium, and methane will purge from liquid to gas as it passes through the oxygen module. This "gas stripping" is the suspected cause of failure.

Gas stripping that reduces the apparent flux of gases was investigated to understand this impact. Results of stripping tests revealed that gas stripping removed 44.7 mg/(min*m²) from solution when oxygen was 2–4 mg/L. This stripping caused a reduction in the effective gas transfer of the system during operation with pure gases. Transfer tests were performed using CLARCOR QP952 modules in series and in parallel to determine if isolating the methane module in a separate loop from the oxygen module would allow better gas transfer. The results for oxygen flux are shown in Figure 4-10. For comparison, the flux for this membrane using pure oxygen gas flow was 382.3 mg/(m²*min).

Using modules in series, the same membrane's flux was reduced by a factor of 3 to 10 depending on the module configuration. The flux difference between the two series configurations can be explained based on what gas was introduced second. After the second module, DO was returned to the reactor, where it distributed throughout the tank volume. The observed final concentration of DO during testing was 50.1% of saturation when oxygen was introduced last or if the modules were operated in parallel, but

only reached 22.5% saturation if oxygen was introduced first in series. Parallel operation results are

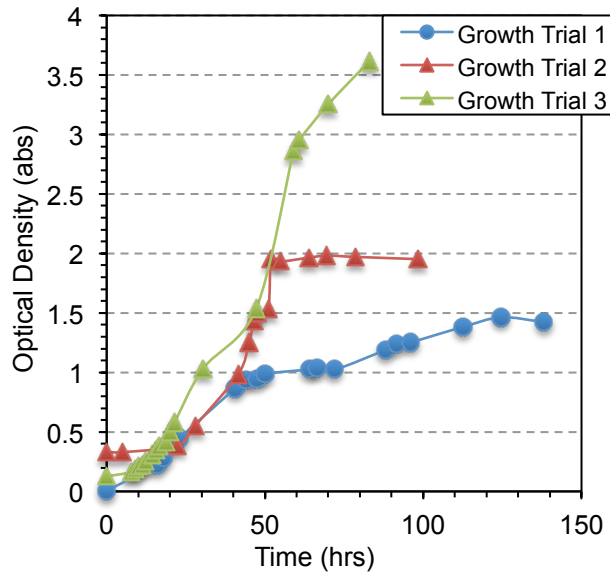


Figure 4-9. A compilation of three bacteria growth trials, where modules were used in series, and PHB was never produced. Circles (growth trial 1) represent measurements using a 20 mL Hach vial and triangles (growth trials 2 and 3) represent OD measurements using a 200- μ L quartz cuvette.

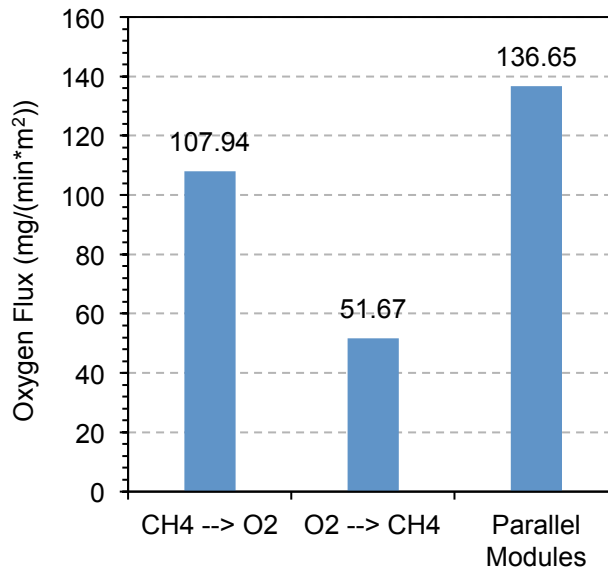


Figure 4-10. Results of effective oxygen flux tests for CLARCOR QP952 membrane used in series and parallel operation with pure oxygen and pure methane in separate modules. Order of gases is denoted on the x-axis. Parallel configuration has modules in separate loops. Calculations used a DO range of 2-4 mg/L.

comparable to oxygen being introduced second. When dissolved gas concentrations enter the reactor from the second module in series, they appear to accumulate more than when they are introduced first. In

parallel operation, each module delivers gases to the reactor; the gases are still stripped when they enter the other loop but are available to bacteria for growth before that occurs.

4.2 Growth Trial with Pure Gases and Flat Sheet Modules in Parallel

According to the results of gas transfer testing, using modules in parallel should allow more effective delivery of both gases to the reactor. Gas transfer testing indicated that liquid flow rate also influenced gas exchange. During trials in parallel, micro-pumps that circulated liquid could control flow independently in the methane and oxygen modules. Liquid flow variation allowed the exchange of one gas or the other to be changed. Stripping is still an issue in this reactor because pure gases were used in each module. To minimize the methane stripping, the liquid flow rate of the oxygen module loop was incrementally increased. Early on in the growth trial, bacterial cultures were not very dense, and did not readily consume the dissolved oxygen present. The concept was to allow the methane loop to operate at 2.0 LPM, ensuring delivery of methane, and begin the trial with the oxygen loop at 0.5 LPM. As the trial progressed, the liquid flow rate the oxygen membrane module loop increased and allowed progressive increases in oxygen gas transfer.

The growth trial depicted in Figure 4-11 and Figure 4-12 achieved an OD of 2.0 abs after completely consuming both nitrogen sources. Oxygen levels were adequately maintained in or near the range of 2–4 mg/L, temperature remained at 30 ± 1 °C, and pH remained neutral.

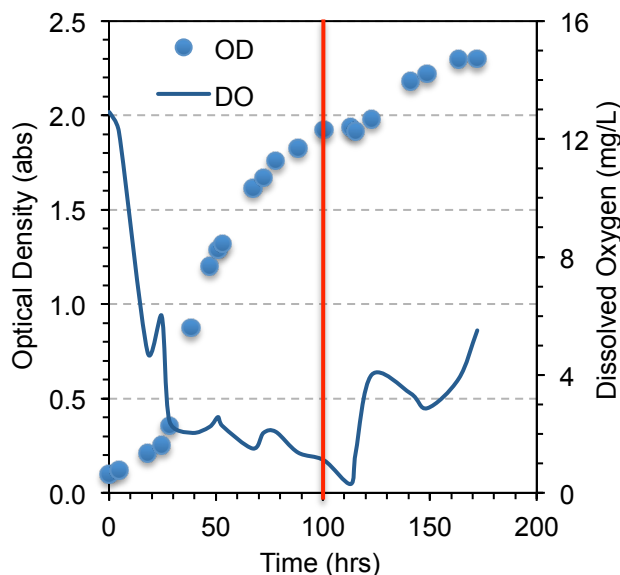


Figure 4-11. Microbial growth measured as OD (blue circles) during a growth trial using pure gases with flat sheet modules in parallel. DO is the dark blue line. Ammonium and nitrate were depleted at 100 hours and is indicated by a red line.

Bacterial growth entered the exponential growth phase at 25 hours, and from then to 113 hours, the DO steadily decreased. Small peaks in DO are time points where the liquid flow rate of the oxygen

loop was increased to maintain DO concentrations of 2–4 mg/L. This method was effective, until growth reached an OD > 1.6 abs. At this point the DO declined, and growth entered a lag phase beginning at the red line. This point occurred at ~100 hours, and Figure 4-12 indicates that was the point when nitrogen sources were depleted, and PHB production would be possible for the bacteria.

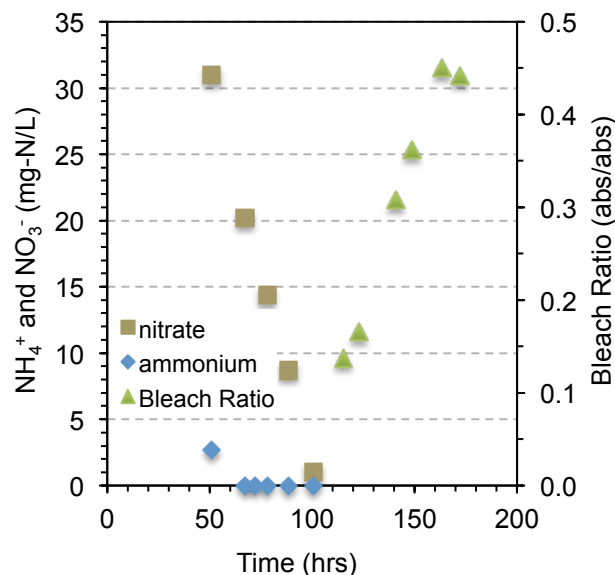


Figure 4-12. Consumption of nitrate and ammonium, and bleach ratio tests performed during the growth trial using pure gases with flat sheet parallel modules. At 100 hours, nitrogen sources are depleted, and PHB production begins.

Growth entered a lag period prior to PHB production, and after 120 hours, the OD increased steadily, attributed to bacteria becoming enlarged due to formation of intracellular PHB. This assertion is strengthened by the fact that nitrate and ammonium were depleted at 100 hrs, the bleach ratio continued to increase steadily, and presence of PHB was confirmed by Mango Materials by FTIR analysis of samples. The final bleach ratio of 0.44 was measured by FTIR to be equivalent to 22% PHB (per mass of dry cells). These results confirm that the growth trial was successful, and that membranes are capable of providing enough gas for bacteria to grow and produce PHB.

4.2.1 PHB Trial without Nitrogen Consumption

To strengthen the confirmation of PHB production, Mango Materials sent a culture that had already consumed all nitrogen sources and was ready to produce PHB. Growth medium was prepared without the addition of ammonium or nitrate, and a growth trial was performed under normal operation, but with the addition of enough of the culture to reach an OD similar to the OD of the previous trial when bacteria began producing PHB. This trial is summarized in Figure 4-13, which depicts the OD, DO, and PHB (confirmed via samples sent to Mango Materials). The trial produced 34.0% PHB (per mass of dry cells), and further confirmed that the reactor provided gas concentrations that resulted PHB production.

This trial and the previous successful trial prove that using membrane modules in a parallel configuration while using pure methane and oxygen gases was a method that produces PHB.

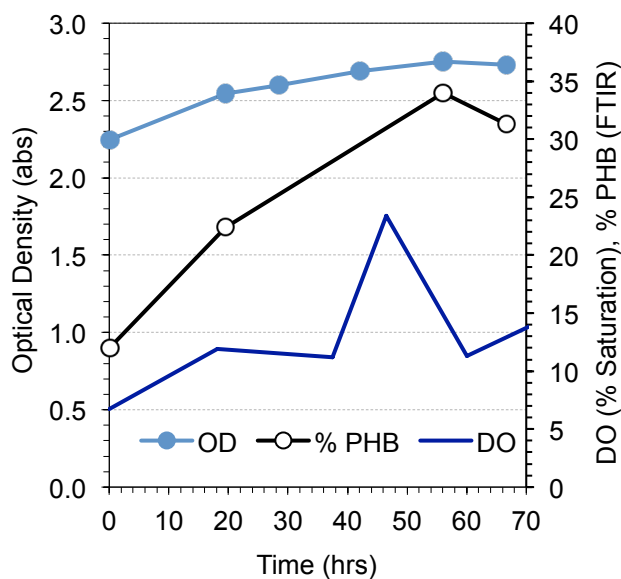


Figure 4-13. Microbial growth measured as OD and PHB production measured by FTIR during a growth trial using pure gases with flat sheet modules in parallel. DO is the dark blue line. Nitrogen sources were absent during this trial, and bacteria were previously grown at Mango Materials.

4.3 Growth Trials with Gas Mixture and Flat Sheet Membrane

Growth and PHB production were successful in the parallel module configuration, but gas stripping occurred during operation because gases were pure in each module. By mixing gases prior to the modules, the fed partial pressures of methane and oxygen can be equal in each module. This eliminates stripping in the modules, but comes at the cost of reducing the gas transfer because each gas has a reduced concentration in the gas stream. Oxygen flux results of the CLARCOR QP952 membrane using a 1:1 (methane:oxygen) gas mixture were calculated at 81.5 mg/(min*m²); compared to 340 mg/(min*m²) when pure oxygen was used. However, because two modules were supplied with the gas mixture, the area for gas transfer was doubled, and neither module stripped gases from solution.

The optimal oxygen concentration range was not maintained during this trial due to reduced partial pressures in the modules and wetting problems due to poor drainage in the FS module. These two factors decreased gas transfer during the trial. The OD and concentration of DO over the course of the growth trials are shown in Figure 4-14.

Henry's law states that the saturation concentration of a gas in solution is directly related to its partial pressure. Saturation for a mixed gas can be calculated based on the partial pressure of the gas in the membrane module gas channel, and a 1:1 gas mixture would result in half of the saturation concentration for a pure gas according to Henry's law. This might decrease the concentration difference between the saturation and observed concentrations in the liquid medium, which, according to Equation

2.2, would also decrease the rate of gas transfer or $K_L a$.

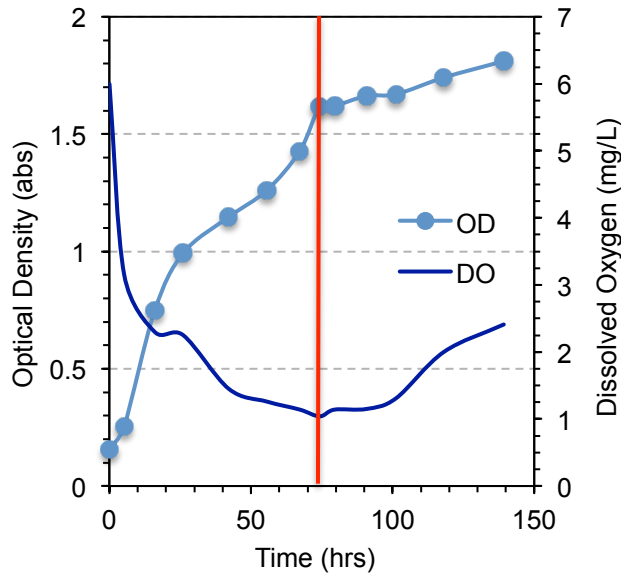


Figure 4-14. Optical density and oxygen concentrations of a growth trial using flat sheet membrane QP952 and a 1:1 methane oxygen gas mixture by volume, in two separate modules, in parallel configuration. Flow rates of both liquid loops were 2.0 LPM. The red line indicates ammonium and nitrate depletion, where PHB production began.

As the bacteria grew and consumed gases in solution, gas transfer was insufficient to maintain DO concentrations, which fell below the desirable DO range of 2–4 mg/L. Bacteria did not appear to be inhibited by this because their growth was comparable to that during the parallel trials that used pure gases, which means that methane and oxygen were available for growth but were readily consumed by the bacteria. Gas transfer was complicated by water vapor condensation in the gas channels of both membrane modules, which reduces gas transfer. Condensation was drained periodically but accumulated again overnight while the system was not attended, slowly decreasing the gas transfer rates. This may have been due to a pinhole leak in the membrane or a faulty seal. However, bacteria still grew and reached an OD of 1.8 abs; this lower OD may be due to the initial concentrations of ammonium and nitrate were 2.5 mM instead of the standard 3 mM, or it may be due to inadequate gas transfer. Figure 4-15 depicts the consumption of ammonium and nitrate, and bleach ratio indicative of PHB production.

This trial depleted the nitrogen sources by 75 hours, after which the bacteria likely began producing PHB. Bleach ratios above 0.1 indicate PHB is likely to have formed, but after 90 hours, one of the membranes became repeatedly inundated with water condensation in the gas channel. The gas mixture flow was connected to both modules, thus, the water present in one of the modules created and increasing resistance in one module's gas channel that eventually caused the gas flow to only pass through the other membrane module. The test was terminated after several bleach ratio measurements confirmed possible decreases in PHB concentrations, and the wetting could not be fixed via tightening or draining the module. The test was still considered successful because nitrogen sources were depleted,

and results of bleach ratios were above 0.1 with a maximum bleach ratio of 0.208, which indicates potential that the bacteria produced PHB in this trial.

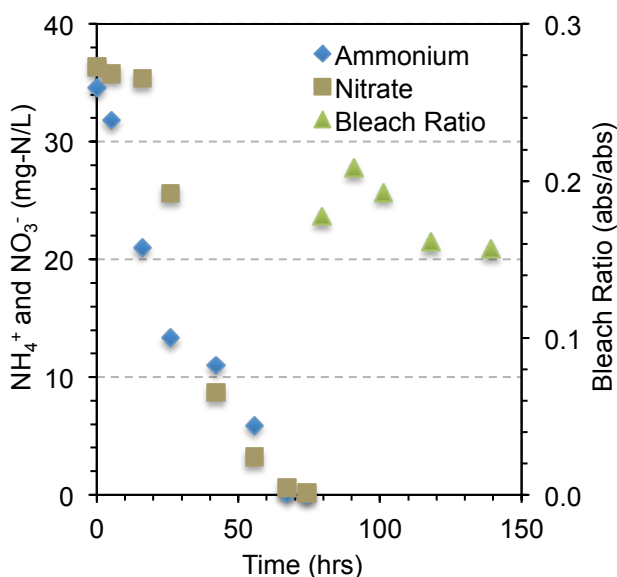


Figure 4-15. Consumption of nitrogen sources by bacteria, and bleach ratio tests for PHB production, in flat sheet QP952 mixed gas growth trial. PHB mode started at ~75 hours.

This trial confirmed that gas mixtures with membranes provide high enough dissolved methane and DO concentrations for bacteria to deplete the nitrogen sources and produce PHB. QP952 membranes allowed water vapor into the gas stream, which condensed and progressively reduced gas transfer; condensation was observed as quickly as 24 hours, but during other tests and growth trials it was not observed at all.

4.4 Growth Trials with Gas Mixture and Hollow Fiber Membrane

Two Minntec HF modules were used in this growth trial for gas transfer instead of the FS module. Draining of the condensate was facilitated during gas mixture trials with HF modules by tilting the modules. This trial used the HF modules to increase the surface area of the membrane and investigate how a higher gas transfer rate (K_La) would impact bacterial consumption of nitrogen sources and PHB production compared to previous FS tests. Growth trial results are depicted in Figure 4-16.

The final OD of this trial was 3.365, the highest of all growth trials performed. After the growth trial was complete, samples were taken from the reactor, diluted to different ODs, and then measured for volatile suspended solids (VSS) to correlate OD to VSS; these results can be found in Appendix D. Nitrogen depletion occurred faster than in any other trial, occurring in 40 hours, versus the 75 and 100 hours to nitrogen depletion observed during the trials using a FS with gas mixture and FS with pure gas, respectively. Nitrogen depletion and bleach ratios are depicted in Figure 4-17. The change in bleach ratio was due to results showing that the digestions were incomplete, thus the 1:9 ratio values are considered

the most accurate for this trial. PHB results via FTIR indicated $28\% \pm 8.5\%$, but the standard deviation was very large because the sample was not homogenized at CSM prior to or after drying. Mango Materials homogenized the sample and tested it using gas chromatography to confirm the actual PHB content was 46.9% (per mass of dry cells).

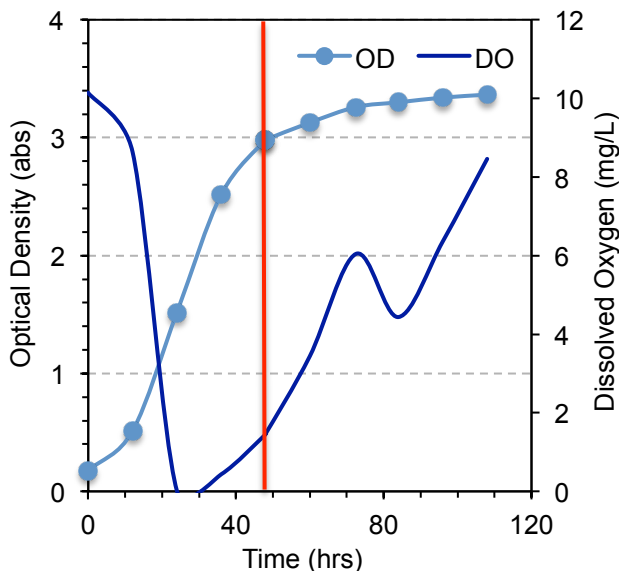


Figure 4-16. Optical density and DO during the growth trial using two Minntec MCV-030 HF modules (0.2323 m^2) with mixed gases. The red line indicates ammonium and nitrate depletion, where PHB production began. DO was depleted after 20 hours due to a conservative gas mixture composition, which was subsequently increased to 1:1 parts methane to oxygen.

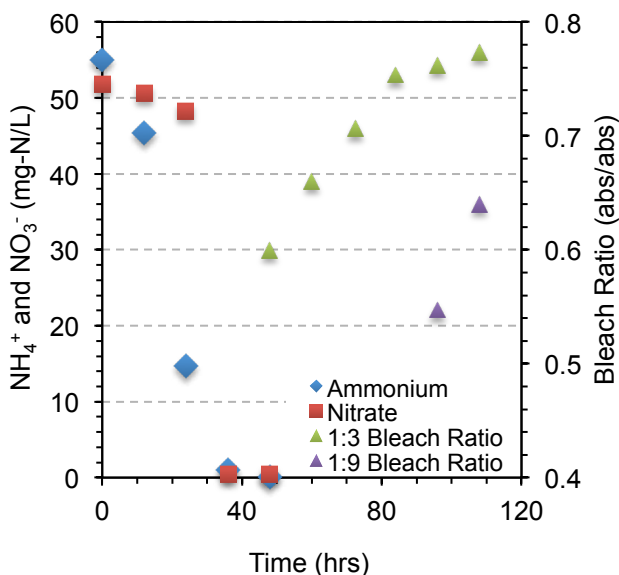


Figure 4-17. Ammonium and nitrate consumption and bleach ratio tests for PHB production, in hollow fiber mixed gas growth trial. PHB production began at ~40 hours. Increased bleach dilutions were used at the end of this trial to compensate for the denser culture produced in this trial.

The increases in growth and PHB production may have resulted from the higher gas transfer rate of the Minntec module due to increased membrane surface area. K_La of the Minntec module is much higher than the QP952 ($12.65 \pm 2.01 \text{ hr}^{-1}$ versus $4.00 \pm 0.11 \text{ hr}^{-1}$). This result suggests that previous membrane and gas configurations may not have provided the bacteria with enough methane to grow at their maximum rate. Multiplying the oxygen fluxes of the QP952 and Minntec membranes by their areas results in mass fluxes of 6.56 mg/min and 17.9 mg/min, respectively. Thus, the dissolution rate of oxygen and methane gases is three times greater with the Minntec module due to its increased surface area. This was accompanied by an increased growth rate and reduced time to deplete nitrogen sources and reach PHB production mode.

Gas mixtures in this trial did not maintain consistent DO concentrations. However, Mango Materials confirmed that during rapid growth, the DO levels are often not maintained because the bacteria use the oxygen too quickly. Increased control over mixtures and a computerized system that monitors and adjusts gas and liquid flows may better support bacterial growth. Drainage of the condensate from the shell of the HF module also reduced the potential for membrane wetting and maintained pore space for gas transfer. Exhaust tubing captured approximately 50 mL of condensate over the course of this trial.

4.5 Discussion of Growth Trials

Each growth trial provided different insights into how membranes may best be applied to grow bacteria and produce PHB. The series configuration of modules using pure gases was plagued by gas stripping and did not produce PHB. The parallel configuration with FS modules did produce PHB using pure gases, but gas stripping still occurred, as did membrane wetting. Mixed gases using FS modules produced PHB, but PHB was not confirmed by FTIR because the trial was terminated due to membrane wetting issues. These issues were mitigated during the HF mixed gas growth trial that was successful in growing bacteria with PHB, and did so in the least amount of time of all the trials performed.

Variables such as initial cell mass from inoculation, initial PHB content of the cells (if any), and initial nitrogen concentration were not consistent, which may have contributed to the different rates of nitrogen consumption. Methane concentrations in solution throughout the trial were unknown, and may also prove to be an influential factor during later studies. All types of growth trials performed are summarized in Table 4-1, which gives values for the time to nitrogen source depletion, initial OD, maximum OD, maximum bleach ratio observed, and PHB confirmed by Mango Materials using FTIR.

Table 4-1. Comparison of Growth Trial Performance

| <i>Membrane/ module config./ gas config.</i> | <i>Initial nitrogen concentration (mg-N/L)</i> | <i>Approx. time to nitrogen depletion (hrs)</i> | <i>Initial Optical Density (abs)</i> | <i>Maximum Optical Density (abs)</i> | <i>Maximum Bleach ratio measured (abs/abs)</i> | <i>PHB per cell mass confirmed (%)</i> |
|--|--|---|--|--|--|--|
| FS/Series/Pure | 84 | N/A | 0.155 | 1.463 | N/A | N/A |
| FS/Parallel/Pure | 84 | 100.6 | 0.1 | 2.30 | 0.45 | 22% |
| FS/Parallel/Mixed | 71 | 75 | 0.155 | 1.811 | 0.208 | N/A |
| HF/Parallel/Mixed | 106.8 | 40 | 0.174 | 3.365 | 0.64 | 46.9% |

PHB measurements were not performed on the bacteria prior to N depletion during growth trials, so the background bleach ratio prior to PHB production is unknown. Also, if PHB was initially in the cells, the rate of nitrogen consumption may have increased due to PHB being readily available as an intracellular carbon source. The shortest time to nitrogen depletion was the trial with the highest initial OD, and the longest time to depletion was the trial with the lowest OD. This indicates that the increased rate of consumption may also be due to the inoculum delivering a higher initial cell mass. In addition, the differences in initial nitrogen concentration may have also changed the rate of nitrogen depletion.

CHAPTER 5

CONCLUSIONS

Use of hollow fiber and flat-sheet membranes for gas transfer successfully maintained concentrations of dissolved methane and dissolved oxygen required by methanotrophic bacteria for growth and production of PHB. Gas transfer testing provided insight on the effectiveness of membranes for this application. The flux observed from the flat-sheet membranes was very promising, as were the gas transfer rates of the hollow fiber modules. Parallel configuration of the membrane modules proved to be the most effective method of gas delivery. Further investigation into the use of hollow fiber modules and spiral wound modules (flat-sheet membranes) within a bench-scale bioreactor system is recommended. Future research needs to address how to manage the water vapor transported through the membrane, what impacts a high density culture will have on the membranes, and how to efficiently use gases within the system, be that mixed gas delivery or pure gases.

5.1 Investigation Summary

Hydrophobic microporous membranes, both flat-sheet and hollow fiber types, are suitable for gas transfer. Flat-sheet membranes produced higher fluxes than the porous hollow fibers by a factor of five (346.1 versus 77.1 mg/(min*m²)). The dense hollow fiber module from PermSelect, with pressure from the oxygen gas driving the gas exchange, was the most promising of the hollow fiber modules with a flux of 155.3 mg/(min*m²). Minntec and Liqui-Cel porous hollow fiber modules, with surface areas of 0.2323 and 1.4 m², respectively, transferred gas at rates of 12.6 to 38.8 hr⁻¹, respectively, which exceeded the flat-sheet gas transfer rate of 3.4 hr⁻¹. Higher surface area of the hollow fiber modules compensated for their low oxygen flux.

Membrane modules utilizing pure methane and oxygen should not be operated in series within a single loop because this configuration caused gas stripping, which reduced the reactor concentration of the dissolved gas fed into the first module in series. Gas concentrations during series operation were insufficient to grow bacteria with intracellular PHB. If modules must use pure gases, they require parallel loops for the membrane modules. Parallel membrane module operations successfully produced PHB during this study. A growth trial using a CLARCOR flat-sheet membrane (QP952) produced intracellular PHB polymer granules measured by FTIR as 22–33% per mass of dry cells, and was produced by supplying pure gases to membrane modules in parallel loops. Growth trials using methane and oxygen gas mixtures (1:1) supplied to the same membrane and module configuration were also successful in producing a surrogate confirmation of PHB, but membrane wetting from water vapor condensation in the gas channel diminished gas exchange and inhibited sustained PHB production. Minntec hollow fiber modules (FiberFlo MCV-030) used for a growth trial with the same gas mixture were arranged to drain condensate from the gas channel; bacteria produced 46.9% PHB (per mass of dry cells) confirmed by GC, and exhibited the most rapid growth of any test during this study.

5.2 Recommendations for Further Research

The results from operation of the bench-scale system presented unsolved problems and additional questions. Optical densities reached by Mango Materials' four-liter system are an order of magnitude higher due to repeated additions of ammonium and nitrate (Mango Materials, 2016). Batches grown in this study only reached OD of 1.8–3.3 abs. Growth of a denser culture will need a computer control system that doses nutrients; maintains temperature and pH; has geared micro-pumps suitable for particle diameters larger than the size of bacteria; manages and maintains methane and oxygen throughout the system; and responds to changes in conditions to maintain optimal growth. Increased culture density may generate increased membrane fouling for this system, and will need to be explored at bench-scale before pilot-scale can become a realistic option. If increased culture density does create membrane fouling, then methods of cleaning the membrane need to be investigated as well.

The surface areas of hollow fiber membranes used in this study were one or two orders of magnitude higher than the flat-sheet membranes. Increasing the surface area of flat sheet modules to match the hollow fiber modules may result in K_La values that match and potentially exceed the gas transfer rates of the hollow fiber modules. Flat-sheet spiral-wound modules should be explored because results indicate they should produce high rates of gas transfer. Water vapor transports via the pores of hydrophobic membranes, which needs to be characterized for the hollow fibers. When that water vapor condenses, it decreases gas transfer, and management methods such as warming gases and condensing water vapor outside of the modules should be investigated as solutions.

Membranes foul during growth trials due to cell attachment or slimes produced by the cells that are deposited onto the membrane, thus plugging pore space and reducing gas transfer of the membrane. These extracellular materials may also degrade the membrane, which should be investigated using scanning electron microscopy. Impacts on the membrane will likely increase as the culture density increases, and was observed during this study as biomass accumulation in the growth media channel and reduced gas transfer, which occurred during the growth trials in this study. However, this study only grew low-density cultures that are not representative of the densities desired for PHB production. Future research also needs to grow cultures at higher densities to prove that this system can be used to produce large enough quantities of PHB that would justify the use of this system.

PHB yield, measured as mass of PHB per mass of substrate, was not calculable using this system. Masses of methane, oxygen, and nutrients required to produce PHB are important to know when considering commercial application of a membrane-based reactor. Mass flow controllers and calibrated dosing systems could be used to accurately determine how much of those materials are used within a growth trial, and allow for a system yield to be calculated. Gas channel concentrations also need to be measured to determine whether gases are depleted within the system, and could be used to optimize their use, thus increasing efficiency. Future research should include using a gas loop where depletion of gases can occur. Yield needs to be known to compare whether this system is more effective than direct gas sparging.

Gas transfer during this study was impacted by flow rates, gas mixture concentrations, available membrane area, biological fouling, and membrane wetting from condensation of water vapor that crossed the membrane via pore space. All of these parameters need to be investigated further with respect to their impact on system operations. This study only characterized gas transfer with respect to oxygen, and assumed methane gas transfer. Gas mixtures were not precise, and require revisiting to confidently report whether they are worthwhile mode of gas delivery. Despite the further need for research, this study provided significant insight into the feasibility of membrane-based bioreactors for PHB production.

REFERENCES CITED

- Amon, T., Amon, B., Kryvoruchko, V., Machmüller, A., Hopfner-Sixt, K., Bodiroza, V., Hrbek, R., Friedel, J., Pötsch, E., Wagentristl, H., Schreiner, M., Zollitsch, W. (2007). Methane production through anaerobic digestion of various energy crops grown in sustainable crop rotations. *Bioresource Technology*, 98(17), 3204–3212. <https://doi.org/10.1016/j.biortech.2006.07.007>
- Anthony, C. (1986). *Bacterial oxidation of methane and methanol*. *Adv Microb Physiol* (Vol. 27). Retrieved June 9, 2017, from http://www.ncbi.nlm.nih.gov/entrez/query.fcgi?cmd=Retrieve&db=PubMed&dopt=Citation&list_uids=3020939
- APHA, AWWA, & WEF (Eds.). (1998). *Standard Methods for the Examination of Water and Wastewater* (18th ed.).
- Augenbraun, H., Matthews, E., & Sarma, D. (2010). The Global Methane Cycle. Retrieved May 29, 2017, from icp.giss.nasa.gov/education/methane/intro/cycle.html
- Barthlott, W., Neinhuis, C., Verlot, H., & Schott, C. L. (1997). Purity of the sacred lotus, or escape from contamination in biological surfaces, 1–8.
- Beaman, J., Bergeron, C., Benson, R., Cook, A.-M., Gallagher, K., Ho, K., Hoff, D., Laessig, S. (2016). *State of the Science White Paper A Summary of Literature on the Chemical Toxicity of Plastics Pollution to Aquatic Life and Aquatic-Dependent Wildlife*.
- Boyle, W. C. (1976). Energy recovery from sanitary landfills—a review. In H. Barnea & J. Schlegel (Eds.), *Microbial Energy Conversion* (pp. 119–138). Pergamon Press, Oxford, UK.
- Cath, T. Y., Adams, V. D., & Childress, A. E. (2004). Experimental study of desalination using direct contact membrane distillation: A new approach to flux enhancement. *Journal of Membrane Science*, 228(1), 5–16. Retrieved June 30, 2017, from <https://doi.org/10.1016/j.memsci.2003.09.006>
- CellTreat. (2014). Chemical Compatibility Guide. Cell Treat Scientific Products. Retrieved June 6, 2017, from [https://www.celltreat.com/sites/default/files/Polypropylene Chemical Compatibility Guide_2014_0.pdf](https://www.celltreat.com/sites/default/files/Polypropylene%20Chemical%20Compatibility%20Guide_2014_0.pdf)
- ChemlinePlastics. (2008). Chemical Resistance Guide. Retrieved June 6, 2017, from https://everythinginsidethefence.com/wpcontent/uploads/chemline_chemical_resistance_guide_205.pdf
- Chisti, Y., & Moo-Young, M. (1989). On the calculation of shear rate and apparent viscosity in airlift and bubble column bioreactors. *Biotechnology and bioengineering*, 34(11), 1391-1392.
- Dębowski, M., Zieliński, M., Grala, A., & Dudek, M. (2013). Algae biomass as an alternative substrate in biogas production technologies - Review. *Renewable and Sustainable Energy Reviews*, 27, 596–604. Retrieved June 30, 2017, from <https://doi.org/10.1016/j.rser.2013.07.029>
- Derraik, J. G. B. (2002). The pollution of the marine environment by plastic debris: A review. *Marine Pollution Bulletin*, 44(9), 842–852. Retrieved June 9, 2017, from [https://doi.org/10.1016/S0025-326X\(02\)00220-5](https://doi.org/10.1016/S0025-326X(02)00220-5)
- Dobroth, Z. T., Hu, S., Coats, E. R., & McDonald, A. G. (2011). Polyhydroxybutyrate synthesis on biodiesel wastewater using mixed microbial consortia. *Bioresource Technology*. Retrieved may 29, 2017, from <https://doi.org/10.1016/j.biortech.2010.11.053>

- Doi, Y., Kanesawa, Y., Tanahashi, N., & Kumagai, Y. (1992). Biodegradation of microbial polyesters in the marine environment. *Polymer Degradation and Stability*. Retrieved May 29, 2017, from [https://doi.org/10.1016/01413910\(92\)90154-W](https://doi.org/10.1016/01413910(92)90154-W)
- Engler, R. E. (2012). The complex interaction between marine debris and toxic chemicals in the ocean. *Environmental Science and Technology*, 46(22), 12302–12315. Retrieved June 16, 2017, from <https://doi.org/10.1021/es3027105>
- EPA, U. S. (2017). Basic Information on Landfill Gas. Retrieved June 16, 2017, from www.epa.gov/lmop/basic-information-about-landfill-gas#one
- Eriksen, M., Maximenko, N., Thiel, M., Cummins, A., Lattin, G., Wilson, S., Hafner, J., Zellers, A., Rifman, S. (2013). Plastic pollution in the South Pacific subtropical gyre. *Marine Pollution Bulletin*, 68(1–2), 71–76. Retrieved June 6, 2017, from <https://doi.org/10.1016/j.marpolbul.2012.12.021>
- Eriksen, M., Theil, M., & Lebreton, L. (2017). Nature of Plastic Marine Pollution in the Subtropical Gyres. In *The Handbook of Environmental Chemistry* (pp. 41–53). Springer Berlin Heidelberg. Retrieved June 6, 2017, from https://doi.org/10.1007/698_2016_123
- Evers, J. (2014). Great Pacific Garbage Patch. Retrieved June 6, 2017, from www.nationalgeographic.org/encyclopedia/great-pacific-garbage-patch/
- Ferrell, R. T., & Himmelblau, D. M. (1967). Diffusion Coefficients of Nitrogen and Oxygen in Water. *J. Chem. Eng. Data*, 12(1), 111–115. Retrieved August 28, 2017, from <https://doi.org/10.1021/je60032a036>
- Golovlev, E. L. (2001). Ecological Strategy of Bacteria: Specific Nature of the Problem. *Microbiology*, 70(4), 379–383. Retrieved June 16, 2017, from <https://doi.org/10.1023/A:1010476507199>
- Gulliver, T. (2017). *Degradation of PHB and PE Microbeads in Aerobic and Anaerobic Biological Wastewater Treatment Microcosms*. Colorado School of Mines.
- HACH. (2005). DR5000 Spectrophotometer Procedures Manuel. Retrieved August 7, 2017, from <https://doi.org/DOC082.98.00670>
- Hemond, H. F., & Fechner, E. L. (2015). *Chemical Fate and Transport in the Environment* (Third Ed.). Elsevier.
- Holmes, P. A. (2002). Applications of PHB - a Microbially Produced Biodegradable Thermoplastic. *Physics in Technology*, 16(1).
- Holophane. (2011). Acrylic & Polycarbonate Compatibility. Acuity Brands Lighting, Inc. Retrieved June 6, 2017, from http://www.holophane.com/hlp_library/brochures/HL-2445.pdf
- Ineos. (2016). *PP chemical resistance guide*. Retrieved August 7, 2017, from [https://doi.org/10.1016/S0026-0576\(98\)80804-0](https://doi.org/10.1016/S0026-0576(98)80804-0)
- IPEX. (2013). *Chemical Resistance Guide*. Retrieved August 7, 2017, from [https://doi.org/10.1016/S0026-0576\(98\)80804-0](https://doi.org/10.1016/S0026-0576(98)80804-0)
- Koutinas, A. A., Xu, Y., Wang, R., & Webb, C. (2007). Polyhydroxybutyrate production from a novel feedstock derived from a wheat-based biorefinery. *Enzyme and Microbial Technology*. Retrieved May 26, 2017, from <https://doi.org/10.1016/j.enzmictec.2006.08.002>
- Kreulen, H., Smolders, C. A., Versteeg, G. F., & van Swaaij, W. P. M. (1993). Microporous hollow fibre

- membrane modules as gas-liquid contactors. Part 1. Physical mass transfer processes. A specific application: Mass transfer in highly viscous liquids. *Journal of Membrane Science*, 78(3), 197–216. Retrieved June 16, 2017, from [https://doi.org/10.1016/0376-7388\(93\)80001-E](https://doi.org/10.1016/0376-7388(93)80001-E)
- Lichtenthaler, F. W. (2010). Carbohydrates as Organic Raw Materials. In *Ullmann's Encyclopedia of Industrial Chemistry*.
- Mango Materials (2016). *Meetings with Mango Materials CTO*.
- Mango Materials (2011). Mango Materials Home Page. Retrieved June 5, 2017, from www.mangomaterials.com
- Matsui, H., & Lee, J. H. (1979). On the measure of the relative detonation hazards of gaseous fuel-oxygen and air mixtures. *Symposium (International) on Combustion*, 17(1), 1269–1280. Retrieved July 21, 2017, from [https://doi.org/10.1016/S0082-0784\(79\)80120-4](https://doi.org/10.1016/S0082-0784(79)80120-4)
- Mevik, B.-H., & Wehrens, R. (2007). The pls Package: Principal Component and Partial Least Squares Regression in R. *Journal of Statistical Software*, 18(2), 144. Retrieved August 21, 2017, from <https://doi.org/10.1063/1.3033202>
- Moore, C. J., Moore, S. L., Leecaster, M. K., & Weisberg, S. B. (2001). A comparison of plastic and plankton in the north Pacific central gyre. *Marine Pollution Bulletin*, 42(12), 1297–1300.
- Nghiem, L. D., & Cath, T. (2011). A scaling mitigation approach during direct contact membrane distillation. *Separation and Purification Technology*, 80(2), 315–322. Retrieved June 30, 2017, from <https://doi.org/10.1016/j.seppur.2011.05.013>
- Pieja, A. J., Sundstrom, E. R., & Criddle, C. S. (2011). Poly-3-hydroxybutyrate metabolism in the type II Methanotroph *Methylocystis parvus* OBBP. *Applied and Environmental Microbiology*. Retrieved May 26, 2017, from <https://doi.org/10.1128/AEM.00509-11>
- Praxair. (2011). Specialty Gases & Equipment Catalog. Danbury, CT: Praxair Technology Inc. Retrieved June 6, 2017, from <http://catalogs.praxairdirect.com/i/25778-specialty-gases-reference-guide/377>
- Praxair. (2016). *Methane, Compressed Safety Data Sheet*. Retrieved June 6, 2017, from www.praxair.com.
- Quééré, D. (2002). Rough ideas on wetting. *Physica A*(313), 32-46. Retrieved June 30, 2017, from <http://www.sciencedirect.com/science/article/pii/S0378437102010336>
- Rishell, S., Casey, E., Glennon, B., & Hamer, G. (2004). Mass transfer analysis of a membrane aerated reactor. *Biochemical Engineering Journal*, 18(3), 159–167. Retrieved June 30, 2017, from <https://doi.org/10.1016/j.bej.2003.08.005>
- Rodhe, H. (1990). A Comparison of the Contribution of Various Gases to the Greenhouse Effect. *Science*. Retrieved May 29, 2017, from <https://doi.org/10.1126/science.248.4960.1217>
- Rostkowski, K. H., Pfluger, A. R., & Criddle, C. S. (2013). Stoichiometry and kinetics of the PHB-producing Type II methanotrophs *Methylosinus trichosporium* OB3b and *Methylocystis parvus* OBBP. *Bioresource Technology*. Retrieved May 26, 2017, from <https://doi.org/10.1016/j.biortech.2012.12.129>
- Sander, R. (2015). Compilation of Henry's law constants (version 4.0) for water as solvent. *Atmospheric Chemistry and Physics*, 15(8), 4399–4981. Retrieved June 30, 2017, from <https://doi.org/10.5194/acp-15-4399-2015>

- Shishkina, V. N., & Trotsenko, Y. A. (1982). Multiple enzymic lesions in obligate methanotrophic bacteria. *FEMS Microbiology Letters*, *13*, 237–242.
- Siddique, R., Khatib, J., & Kaur, I. (2008). Use of recycled plastic in concrete: A review. *Waste Management*, *28*(10), 1835–1852. Retrieved June 9, 2017, from <https://doi.org/10.1016/j.wasman.2007.09.011>
- Siljanen, H. M. P., Saari, A., Bodrossy, L., & Martikainen, P. J. (2012). Seasonal variation in the function and diversity of methanotrophs in the littoral wetland of a boreal eutrophic lake. *FEMS Microbiology Ecology*, *80*(3), 548–555. Retrieved June 30, 2017, from <https://doi.org/10.1111/j.15746941.2012.01321.x>
- Spiegel, R. J., & Preston, J. L. (2000). Test results for fuel cell operation on anaerobic digester gas. *Journal of Power Sources*, *86*(1), 283–288. Retrieved August 21, 2017, from [https://doi.org/10.1016/S0378-7753\(99\)00461-9](https://doi.org/10.1016/S0378-7753(99)00461-9)
- Teuten, E. L., Saquing, J. M., Knappe, D. R. U., Barlaz, M. A., Jonsson, S., Bjorn, A., Rowland, S. J., Thompson, R. C., Galloway, T. S., Yamashita, R., Ochi, D., Watanuki, Y., Moore, C., Viet, P. H., Tana, T. S., Prudente, M., Boonyatumanond, R., Zakaria, M. P., Akkhavong, K., Ogata, Y., Hirai, H., Iwasa, S., Mizukawa, K., Hagino, Y., Imamura, A., Saha, M., Takada, H. (2009). Transport and release of chemicals from plastics to the environment and to wildlife. *Philosophical Transactions of the Royal Society B: Biological Sciences*, *364*(1526), 2027–2045. Retrieved June 16, 2017, from <https://doi.org/10.1098/rstb.2008.0284>
- Tollefson, J. (n.d.). “Flaring” wastes 3.5% of world’s natural gas. Retrieved June 9, 2017, from www.nature.com/news/flaring-wastes-3-5-of-world-s-natural-gas-1.19141
- Toolbox, E. (2017). Altitude Above Sea Level and Air Pressure. Retrieved May 13, 2017, from http://www.engineeringtoolbox.com/air-altitude-pressure-d_462.html
- Vanneste, J., Bush, J. A., Hickenbottom, K. L., Marks, C. A., & Cath, T. Y. (2017). Novel thermal efficiency-based model for determination of thermal conductivity of membrane distillation membranes. *Journal of Membrane Science*.
- Witherspoon, P. A., & Saraf, D. N. (1965). Diffusion of Methane, Ethane, Propane, and n-Butane in Water from 25 to 43°. *Journal of Physical Chemistry*, *69*(11), 3752–3755. Retrieved August 28, 2017, from <https://doi.org/10.1021/j100895a017>
- Zheng, Q., & Lü, C. (2014). Size effects of surface roughness to superhydrophobicity. *Procedia IUTAM*, *10*, 462–475. Retrieved June 30, 2017, from <https://doi.org/10.1016/j.piutam.2014.01.041>

APPENDIX A

The membrane-based bioreactor operates within a fume hood on a platform, and is pictured in Figure A-1.

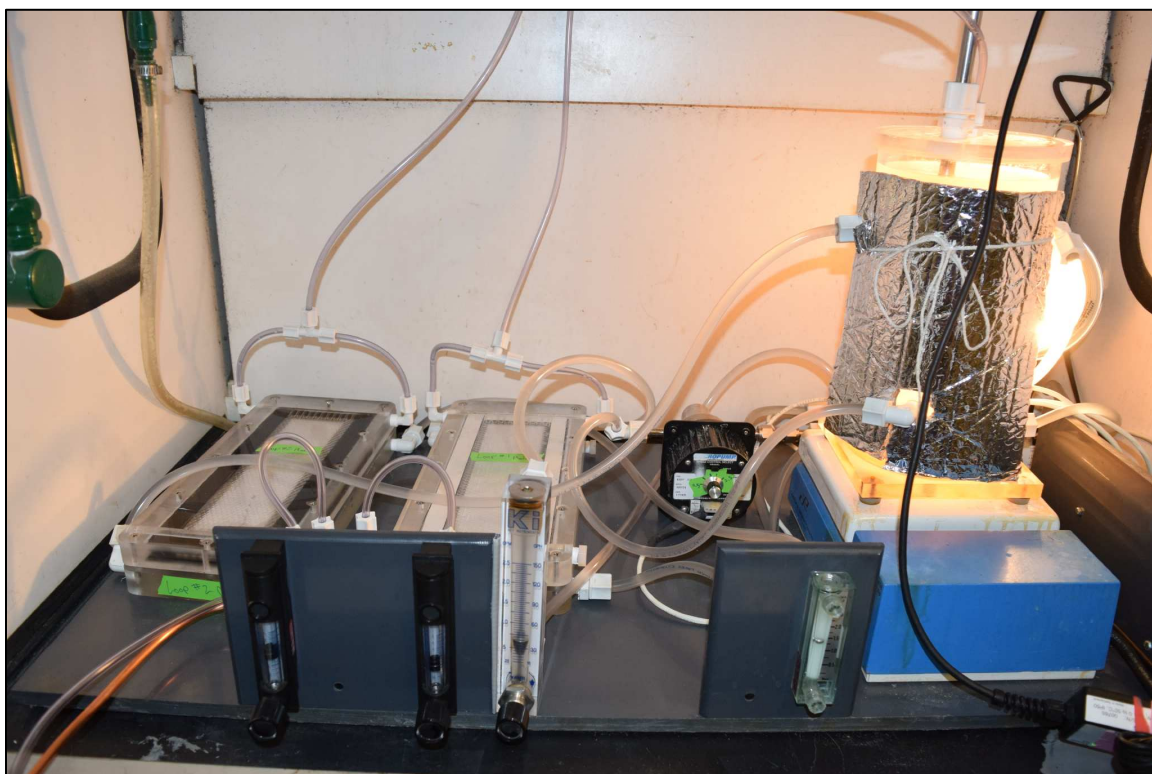


Figure A-1. Membrane-based bioreactor operating with two flat-sheet modules during a growth trial.

In figure A-1, all components of the reactor are visible. Flat-sheet membrane modules were connected to the central tank reactor via two parallel loops, and either methane or oxygen flowed through the gas channel. The black flow meters at the front controlled methane and oxygen flows, and the clear or green rotameter measured the pump flowrate controlled by the black gear pumps. The central tank of the reactor was insulated with reflective bubble wrap, and was warmed by the infrared heating lamp in the back right corner behind it. Two polyethylene tubes directed gas exhaust from the modules upwards and out the rear of the fume hood to isolate the heat lamp and prevent any combustion. The stir plate (blue platform) below the reactor spun the magnetic stir bar inside the reactor.

APPENDIX B

The hollow fiber modules were tested by pumping liquid through the shell space of the module or the lumen of the fiber during separate trials. Figure B-1 depicts the Minntec hollow fiber module being tested with liquid flow in the lumen and in the shell under different flow rates.

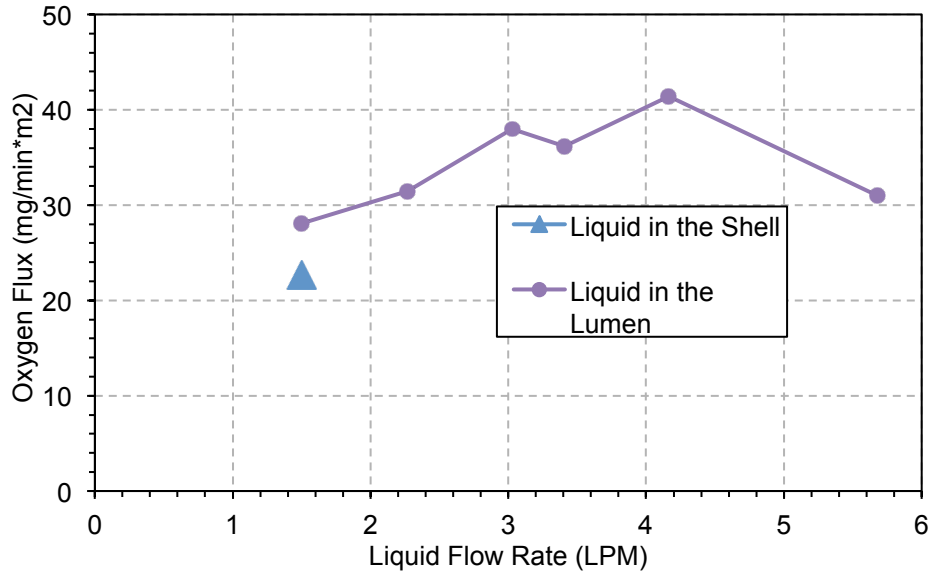


Figure B-0-1. Gas transfer testing using hollow fiber module from Minntec. Liquid was either passed through the lumen (circles) or the shell (triangle) using different liquid flow rates.

The flux results of this test are not accurate or relevant in this case. The relevance of this graph is that when liquid flowed through the shell, the liquid flow rate reached 1.5 LPM when the maximum liquid pressure occurred (30 psig). When the liquid was flowing through the lumen, the flow rate could be substantially increased in comparison. Due to these results, the gas transfer tests in this study were all performed with liquid flows in the lumen.

APPENDIX C

Gas flow variation was also performed in conjunction with liquid flow variation. However, membrane flux was significantly lower than that observed in other tests, which may have resulted from membrane wetting. Flux and K_La results were much lower than expected at similar liquid flow rates, the same gas flow rate, and the same membrane. Due to this, these data were not included in the results section, as they were not considered reliable. However, the results of this test are summarized in Figure C-1.

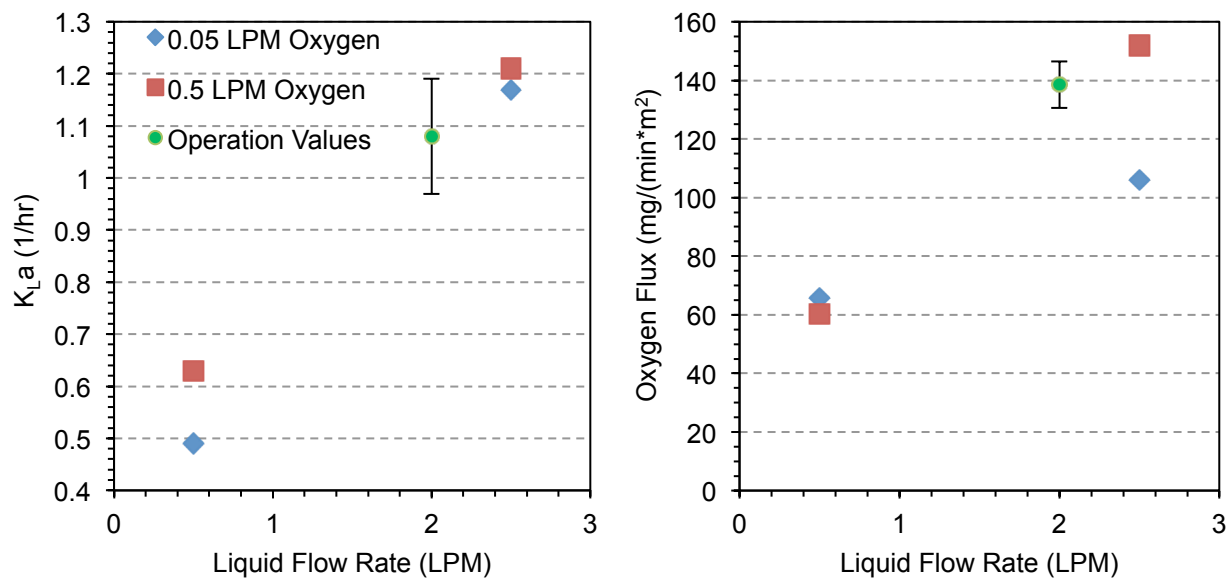


Figure C-0-1. K_La (left) and flux (right) for FS QP952 under different oxygen gas and liquid flow rates; temperature was maintained at 30 °C. Error bars represent standard deviation based on three tests.

Flux and K_La results for this membrane without evident wetting at 2.5 LPM liquid flow and 0.5 LPM oxygen flow were around 400 mg/(min*m²) and 4 hr⁻¹ (Figure 4-8). These values were reduced by a factor of three in the trials with suspected membrane wetting.

APPENDIX D

Optical density is a measurement indicating microbial growth but does not specifically measure how many cells are present or the cell mass, so a correlation was developed between volatile suspended solids (VSS) and OD. To do this, OD and VSS measurements were performed using suspended growth culture from the HF mixed gas growth trial. VSS was measured following Method 2450 from Standard Methods for the Examination of Water and Wastewater (1998), except that a 4.7 cm glass microfiber filter paper rated to 0.7 μm (Whatman 1825-047) was used to capture bacteria. Prior to the VSS measurement, the OD of each sample was measured. These measurements were used to create the correlation curve depicted in Figure D-1 between OD in absorbance at 595 nm and VSS in mg/L.

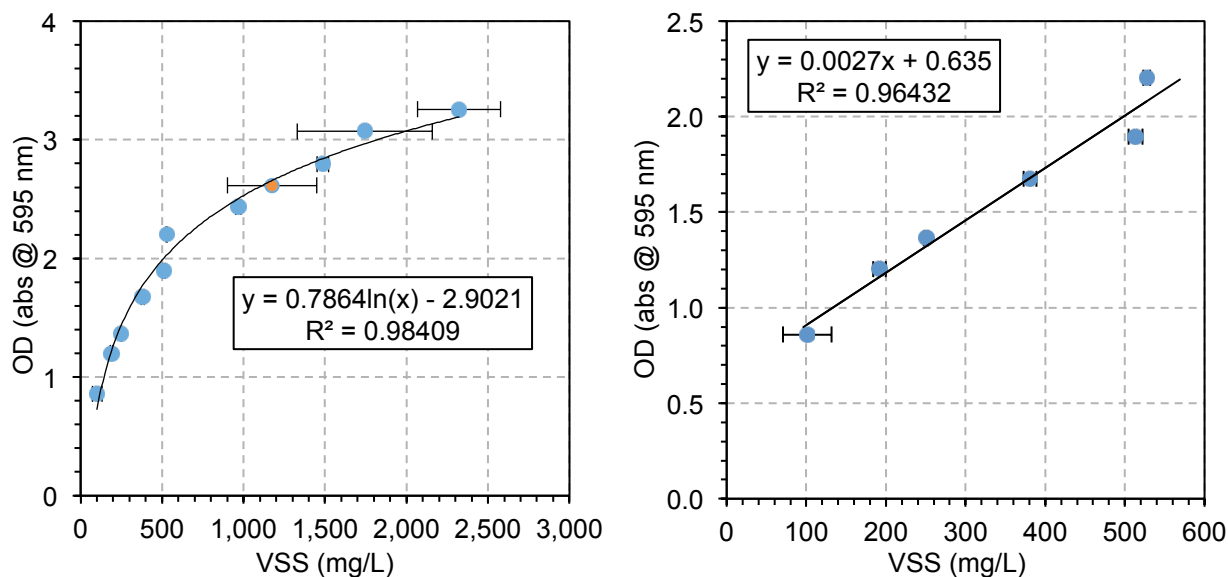


Figure D-0-1. Optical density and VSS measurements are correlated. Graph on the left uses the entire data set and uses a logarithmic trend; graph on the right uses data that appeared linear and uses a linear trend. The bacterial culture was obtained from the growth trial that used hollow fiber modules and gas mixture. Samples were diluted to different ODs and filtered afterwards. Error bars represent the standard deviation of three samples.

The optical density measurements show typical saturation behavior, with OD deviating from linearity with increasing VSS above and OD of approximately 2, though HACH indicates that the DR5000 does not saturate until after 3.5 abs (HACH, 2005). In addition, the VSS measurements became quite variable after the OD exceeds ~ 2.5 , as indicated by an increased in standard deviation.